

ACCEPTED VERSION

Periasamy, Agalya; Shadiac, Nadim Baraket; Amalraj, Amritha; Garajova, Sona; Nagarajan, Yagnesh; Waters, Shane; Mertens, Haydyn D. T.; Hrmova, Maria
[Cell-free protein synthesis of membrane \(1,3\)-beta-D-glucan \(curdlan\) synthase: Co-translational insertion in liposomes and reconstitution in nanodiscs](#)
Biochimica et Biophysica Acta-Biomembranes, 2013; 1828(2):743-757

© 2012 Elsevier Inc. All rights reserved.

NOTICE: this is the author's version of a work that was accepted for publication in *Biochimica et Biophysica Acta-Biomembranes*. Changes resulting from the publishing process, such as peer review, editing, corrections, structural formatting, and other quality control mechanisms may not be reflected in this document. Changes may have been made to this work since it was submitted for publication. A definitive version was subsequently published in *Biochimica et Biophysica Acta-Biomembranes*, 2013; 1828(2):743-757. DOI: [10.1016/j.bbamem.2012.10.003](https://doi.org/10.1016/j.bbamem.2012.10.003)

PERMISSIONS

<http://www.elsevier.com/journal-authors/author-rights-and-responsibilities#author-posting>

Elsevier's AAM Policy: Authors retain the right to use the accepted author manuscript for personal use, internal institutional use and for permitted scholarly posting provided that these are not for purposes of **commercial use** or **systematic distribution**.

21 August 2013

<http://hdl.handle.net/2440/78426>

**Cell-free protein synthesis of membrane (1,3)- β -D-glucan (curdlan) synthase:
co-translational insertion in liposomes and reconstitution in nanodiscs**

**Agalya Periasamy^{a,d}, Nadim Shadiac^{a,d}, Amritha Amalraj^a, Soňa Garajová^{a,c}, Yagnesh
Nagarajan^a, Shane Waters^a, Haydyn D.T. Mertens^b, Maria Hrmova^{a,*}**

^a Australian Centre for Plant Functional Genomics, School of Agriculture, Food and Wine,
University of Adelaide, Waite Campus, Australia

^b Australian Synchrotron, SAXS/WAXS Beamline, 800 Blackburn Road, Victoria, Australia

^c Permanent address: Institute of Chemistry, Centre for Glycomics, Slovak Academy of Sciences,
Slovak Republic

^d These two authors have contributed equally to this work.

* Corresponding author at Australian Centre for Plant Functional Genomics, School of
Agriculture, Food and Wine, University of Adelaide, Waite Campus, Glen Osmond, SA 5064,
Australia. Tel.: +61 8 8313 7160; fax: +61 8 8313 7102; E-mail address:
maria.hrmova@adelaide.edu.au.

Abbreviations: β -OG, *n*-octyl- β -D-glucopyranoside; Brij-58 polyoxyethylene-(20)-cetyl-ether (C1620); CAZy, Carbohydrate-Active enZymes; CF, cell-free; CFPS, cell-free protein synthesis; CHAPS, 3-[(3-cholamidopropyl)dimethylammonio]-1-propanesulfonate; CM, catalytic module; CMC, critical micellar concentration; CrdS, curdlan synthase; DDM, *n*-dodecyl- β -D-maltoside; DM, *n*-decyl- β -D-maltoside; DMPC, 1,2-dimyristoyl-*sn*-glycero-3-phosphocholine; DOPC, 1,2-dioleoyl-*sn*-glycero-3-phosphocholine; DOPG, 1,2-dioleoyl-*sn*-glycero-3-phospho-(1' *rac*-glycerol); DOTAP, 1,2-dioleoyl-3-trimethylammonium-propane; DTT, dithiothreitol; EC, Enzyme Commission; EDTA, ethylenediaminetetraacetic acid; GT, glycoside transferase(s); IMAC, Immobilized Metal Affinity Chromatography; IFT, indirect Fourier transformation; MALDI-TOF, Matrix-Assisted Laser Desorption Ionization-Time of Flight; MS, Mass Spectrometry (spectra); M_r , relative molecular mass; MSP, Membrane scaffold protein; NP 40, nonylphenyl-polyethylene-glycol; PDB, Protein Data Bank; POPC, 1-palmitoyl-2-oleoyl-*sn*-glycero-3-phosphocholine; POPE, 1-palmitoyl-2-oleoyl-*sn*-glycero-3-phosphoethanolamine; PVDF, polyvinylidene fluoride; SAXS, small-angle X-ray scattering; SDS-PAGE, sodium dodecyl sulphate-polyacrylamide gel electrophoresis; SEC, size-exclusion chromatography; SMA, styrene maleic acid; SUMO, small ubiquitin-related modifier; TBS, Tris buffer containing NaCl; Triton X-100, polyethylene-glycol-p-1,1,3,3-tetramethyl-butylphenyl-ether; Tween 80, polyoxyethylene-sorbitan-monolaurate 80; TEM, transmission electron microscopy; TEV, Tobacco Etch Virus; UDP-glucose, uridine-diphosphate glucose; WG-CFPS, wheat germ cell-free protein synthesis; YPD, yeast extract-peptone-dextrose; 3D, three-dimensional.

Abstract

A membrane-embedded curdian synthase (CrdS) from *Agrobacterium* is believed to catalyse a repetitive addition of glucosyl residues from UDP-glucose to produce the (1,3)- β -D-glucan (curdian) polymer. We report wheat germ cell-free protein synthesis (WG-CFPS) of full-length CrdS containing a 6xHis affinity tag and either Factor Xa or Tobacco Etch Virus proteolytic sites, using a variety of hydrophobic membrane-mimicking environments. Full-length CrdS was synthesized with no variations in primary structure, following analysis of tryptic fragments by MALDI-TOF/TOF mass spectrometry. Preparative scale WG-CFPS in dialysis mode with Brij-58 yielded CrdS in mg per ml quantities. Analysis of structural and functional properties of CrdS during protein synthesis showed that CrdS was co-translationally inserted in DMPC liposomes during WG-CFPS, and these liposomes could be purified in a single step by density gradient floatation. Incorporated CrdS exhibited a random orientation topology. Following affinity purification of CrdS, the protein was reconstituted in nanodiscs with *E. coli* lipids or POPC and a membrane scaffold protein MSP1E3D1. CrdS nanodiscs were characterised by small-angle X-ray scattering using synchrotron radiation and the data obtained were consistent with insertion of CrdS into bilayers. We found CrdS synthesised in the presence of the Ac-AAAAAAD surfactant peptide or co-translationally inserted in liposomes made from in *E. coli* lipids to be catalytically competent. Conversely, CrdS synthesised with only Brij-58 was inactive. Our findings pave the way for future structural studies of this industrially important catalytic membrane protein.

Key Words: Family GT2 transferase, small-angle X-ray scattering, surfactants, surfactant peptides, topology, (1,3)- β -D-glucan.

Introduction

The bacterial (1,3)- β -D-glucan, also known as curdlan, is an extracellular polysaccharide that is important for cell structure and physiology of prokaryotic *Agrobacterium* sp [1]. Curdlan has extensive practical and commercial applications in food, cosmetic, pharmaceutical and building industries as previously outlined [1-3]. However, despite the obvious significance of curdlan, the molecular mechanisms that underlie its biosynthesis have not been described at the molecular levels [2,3].

The molecular genetics of curdlan production by *Agrobacterium* sp. has been extensively studied [1-3]. Curdlan synthases (CrdS) [UDP-glucose: (1,3)- β -D-glucan 3- β -D-glucosyltransferase; EC 2.4.1.34] are confined within cell membranes. Based on the sequence homology with other β -glucan synthases, namely plant cellulose synthases, the CrdS enzyme has been classified by CAZy in the GT2 family of glycosyl transferases [3,4]. The cDNA of CrdS from *Agrobacterium* sp. [1] translates into a protein of 654 amino acid residues. Bioinformatics evaluations predict that CrdS has a N_{out}-C_{in} topology, harbours seven membrane spanning α -helices and contains a single large cytoplasmic region inserted between the 3rd and 4th membrane α -helices [2], representing a putative catalytic module (CM). CM contains characteristic catalytic and substrate binding signatures Asp, Asp, Asp (D, D, D) and GlnxxArgTrp (QxxRW) found in other glucosyltransferases classified in the GT2 family [1-4]. CrdS is predicted to contain at least one pair of bonded cysteines located in CM, although the existence of this disulphide bridge is not supported by experimental evidence [2]. The 3D structures of the GT2 enzymes elucidated by X-ray crystallography comprise a soluble bacterial spore-coat protein [5], a chondroitin polymerase enzyme from *Escherichia coli* [6] involved in synthesis of chondroitin sulfate, a putative glycosyltransferase from *Bacteroides fragilis* [Protein

Data Bank (PDB) accession 3BCV, Polani, Kumaran, Burley and Swaminathan, unpublished data] and a recently determined teichoic acid polymerase from *Staphylococcus epidermidis* [7].

Previously, cDNA encoding CM of CrdS cloned into the pET-32a(+) vector containing thioredoxin, and into the ChampionTM pET SUMO system containing a SUMO (small ubiquitin-related modifier) coding region enabled high yield expression of CM, in the form of inclusion bodies [2]. The former vector was chosen because it is recognized to facilitate disulfide bond formation in the reducing environment of *E. coli* [8], alleviates toxic effects of recombinant protein production on host cells, prevents target proteins from proteolytic degradation and accelerates expression of proteins in a soluble form [9]. The inclusion bodies produced in *E. coli* were refolded using a range of buffers and non-surfactant sulfobetaines [2]. Refolded, chimeric CM was found to be inactive, although it showed a native-like circular dichroism spectrum [2].

The objective of the present work was to produce full-length CrdS through a eukaryotic wheat germ cell-free (CF) protein synthesis (WG-CFPS) expression system that enables rapid production of proteins [10]. CFPS systems based on cellular extracts, have emerged recently as efficient and versatile tools for the production of complex integral membrane proteins. Here, the entire process of protein production encompassing transcription and translation steps takes place *in vitro* [12-15]. The CFPS systems overcome many of the technical hurdles of *in vivo* membrane protein production as cell viability and protein production are essentially decoupled [14,16]. The CF systems, not being enclosed by a membrane are open and accessible, and allow supplementation of target-specific additives such as stabilizers, substrates, ligands, chaperones, surfactants and other components at any time during a CF reaction [16-17]. Moreover, the option to co-translationally insert membrane proteins directly into artificial hydrophobic environments often eliminates a need for reconstitution of membrane proteins into lipid environments [18]. In the past twenty years, a variety of extracts,

configurations and expression modes have been established, developed and perfected [19]. WG-CFPS has been used for synthesis of mainly radio-labelled polypeptides in the past and only in recent years has substantial progress in protein yields of membrane and multi-domain proteins been achieved [10,11]. This progress has been primarily due to the removal of components causing damage to ribosomes and mRNA, so CFPS can be sustained for several days provided reaction substrates are replenished [19,20]. Last but not least, robotic automation of WG-CFPS has been achieved with the advent of robotised synthesisers and associated technical progression [21,22].

Our work with recombinant CrdS is aimed at a long-term goal to determine the three-dimensional (3D) structure of this integral membrane protein. In the previous work, the full-length form of CrdS was not produced in the *E. coli* host and only truncated forms were obtained [2]. This led us to explore new approaches towards stable expression of full-length CrdS. We became interested in deployment of particular avenues, such as co-translational insertion of CrdS in liposomes and application of nanodiscs. The emergence of nanodiscs as a tool to study structural aspects of membrane proteins in a near-native environment has gained considerable interest in the past decade [23,24]. During, the process of spontaneous nanodisc self-assembly, the surfactant-solubilised membrane protein becomes surrounded by an annular lipid-bilayer patch, which is held together by a recombinant membrane scaffold protein (MSP). Following purification by size-exclusion chromatography (SEC), a uniform population of soluble, stable and correctly assembled membrane protein occupied nanodiscs is usually obtained [23,24].

In the current work, full-length CrdS was sub-cloned into the pEU-EO1TM plasmids for WG-CFPS, containing a 6xHis affinity tag and either Tobacco Etch Virus (TEV) or Factor Xa proteolytic sites. We investigated bilayer and dialysis modes of WG-CFPS and assessed yields of CrdS in the presence of a range of surfactants and surfactant peptides. Following co-translational insertion of

CrdS in artificial liposomes, we demonstrated single-step purification by floatation through density gradient ultra-centrifugation. Furthermore, with the goal of structural studies, we assembled and purified CrdS nanodiscs to near homogeneity in two distinct lipid environments and characterised them by small-angle X-ray scattering (SAXS) using synchrotron radiation [25]. Synthesised CrdS was analysed by Matrix-Assisted Laser Desorption Ionization-Time of Flight Mass Spectrometry (MALDI-TOF/TOF MS) and assayed for catalytic activity.

Materials and methods

Chemicals and reagents

The sources of oligonucleotide primers, restriction and DNA-modifying enzymes, plasmid extraction kits, EDTA-free Complete Protease Inhibitor Cocktail tablets and other chemicals were described previously [2]. All lipids, except asolectin (Sigma, St. Louis, MO, USA) were purchased from Avanti Polar Lipids (Alabaster, AL, USA).

Recombinant plasmid construction

The full-length coding region of CrdS was amplified by PCR using the 5' primer pairs (Table 1) from the pVS1512 plasmid of an 8.8 kb *EcoRI* *Agrobacterium* genomic fragment containing the *crdASC* genes [2]. The amplified fragments were cloned into the pGEM-T Easy vector system (Promega, Madison, WI, USA). For DNA amplifications the *E. coli* strain DH5 α (Invitrogen, Carlsbad, CA, USA) was transformed with pGEM-His-CrdS, pGEM-His-TEV-CrdS and pGEM-His-Xa-CrdS constructs as recommended by the manufacturer. The plasmids were isolated and digested with *XhoI* and *NotI*, and the CrdS DNA fragments were sub-cloned in-frame into the pEU-

EO1-HIS-TEV-MCSTM vector (CellFree Sciences, Tsurumi-ku, Yokohama, Japan) to generate the pEU-His-CrdS and pEU-His-TEV-CrdS constructs, and into the pEU-EO1-MCSTM vector (CellFree Sciences) to yield the pEU-His-Xa-CrdS construct. The three expression plasmids were transformed into the *E. coli* strain DH5 α cells and the plasmid DNA was sequenced in both directions.

Wheat Germ Cell-Free Protein Synthesis of CrdS

Wheat Germ Cell-Free Protein Synthesis (WG-CFPS) of CrdS was performed sequentially through the uncoupled transcription and translation reactions. Care was taken to prevent RNase contamination throughout by using RNase-free water (MP Biomedicals, Fountain Parkway Solon, Ohio, USA) and RNase AWAY[®] (Molecular BioProducts, San Diego, CA, USA) to sanitise the workspace.

Preparation of plasmid DNA - DNA was isolated from the *E. coli* cells transformed with the pEU-His-CrdS, pEU-His-TEV-CrdS and pEU-His-Xa-CrdS constructs using the PureYieldTM Plasmid Miniprep System (Promega). The quality of purified DNA, expressed as A_{260}/A_{280} was within a range of 1.8-2.0. The DNA was used at a concentration of 1 $\mu\text{g}/\mu\text{l}$.

Transcription (preparation of mRNA) - Plasmid DNA of the pEU-His-CrdS, pEU-His-TEV-CrdS and pEU-His-Xa-CrdS constructs (2.5 μg) was combined with a transcription buffer (CellFree Sciences) and the nucleotide-tri-phosphate (NTP) mix (ATP, CTP, GTP, UTP each at 3 mM) (Roche, Indianapolis, USA), SP6 RNA polymerase (1 U/ μl) (Promega), RNasin (1 U/ μl) (Promega) and RNase free water (MP Biomedicals) were added to a total volume of 25 μl [20]. Synthesis of mRNA proceeded at 42°C for 2.5 hours. The quality of synthesised mRNA was confirmed by 1% (w/v) agarose gel electrophoresis.

Translation (synthesis of CrdS) - Translation was performed through either bilayer mode in the 150 μl total reaction volume or through dialysis mode of 50 μl internal reaction volumes, in a Slide-A-

Lyser Mini dialysis cup, molecular mass cut-off 10 kDa (Thermo Scientific, Rockford, IL, USA). The translation reactions were setup in the dialysis buffer (CellFree Sciences) containing 0.3 mM L-amino acids (CellFree Sciences) with 10 µl mRNA per 25 µl reaction mix. Translation reactions contained the WEPRO wheat germ extract (6.3 µl per 25 µl) (CellFree Sciences), creatine-phosphokinase (0.4 µg/µl) (Roche) and RNase free water (MP Biomedicals). Biotinylated tRNA (1.5 µl/25 µl) (Promega) was added during translation in specific cases to allow for detection of CrdS through a streptavidin-coupled assay. The synthesis in bilayer mode was carried out as described [26] at 20°C for 20 hours, and the synthesis in dialysis mode proceeded according to [20] at 20°C for up to 72 hours, with the supply of a fresh dialysis buffer after 24 hour time intervals. The translation mixture in dialysis mode was placed in dialysis cups and suspended in a buffer reservoir containing 0.6 ml of the dialysis buffer (CellFree Sciences). The translation reaction mixture was supplemented with surfactants, surfactant peptides, amphipols and liposomes, prepared as specified below.

CrdS synthesis with surfactants - Nonionic and zwitterionic surfactants of alkyl-glycosides, steroids, polyoxyethylene-alkyl-ethers, polyethyleneglycol and long-chain phosphoglycerol derivatives were tested above their critical micellar concentrations (CMC) in translation reactions. The list of surfactants, their concentrations and sources are summarised in Table 2.

CrdS synthesis with surfactant peptides - The CrdS synthesis proceeded with 1, 2 and 4 mM concentrations of the acetylated Ac-AAAAAAD (Ac-Ala-Ala-Ala-Ala-Ala-Ala-Asp), Ac-IIID (Ac-Ile-Ile-Ile-Asp) and Ac-LLLK-NH₂ (Ac-Leu-Leu-Leu-Lys-NH₂) surfactant peptides. The peptides were synthesised by Mimotopes (Clayton, Victoria, Australia) and dissolved in RNase free water (MP Biomedicals) to prepare 50 mM stock concentrations.

CrdS synthesis with amphipols - CrdS synthesis proceeded with amphipol A8-35 (Anatrace, Santa Clara, CA, USA) and styrene maleic acid (SMA) at concentrations ranging from 0.5% to 4%. SMA was kindly provided by Dr Timothy Knowles (University of Birmingham, UK).

CrdS synthesis with liposomes - The synthesis of CrdS proceeded with liposomes prepared at final lipid concentrations of 2.5 mg/ml, 5 mg/ml and 10 mg/ml either by using a single lipid component or a mixture of lipids; in the latter case DOPG was mixed with POPE in a 2:3 ratio, by weight. The list of lipids used, their formulae and sources are given in Table 3. CrdS quantification was performed using the ImageJ software [27] from scanned Western blot images. A CrdS calibration curve was based on known amounts of BSA. The liposomes were prepared as follows. The pre-weighed lipid powder in a glass-tube was dissolved in chloroform and dried on a rotary evaporator followed by purging with a stream of nitrogen to remove chloroform. The resultant lipid coating in the glass test-tube was dried for two hours under *vacuo* to remove every trace of chloroform. The dried lipid film was dissolved in the lipid re-hydration buffer (25 mM HEPES, 100 mM NaCl, pH 7.5) to a final concentration of 100 mg/ml. The tube was constantly agitated until dissolved and was kept above the transition temperature of a particular lipid, which varied between -20°C and 23°C. The suspension was extruded 21 times, above the lipid transition temperature, using the Avestin Liposofast extruder (Avestin, Ontario, Canada) through polycarbonate filters with pore sizes of 100 or 400 nm to produce a population of unilamellar liposomes.

Purification of CrdS proteo-liposomes through floatation on Accudenz gradient

A 75 µl aliquot taken from a WG-CFPS translation reaction containing liposomes was mixed with 75 µl of 80% (w/v) Accudenz (Accurate Chemical and Scientific, Westbury, NY) prepared in 25 mM HEPES, pH 7.5, containing 100 mM NaCl and 10% (v/v) glycerol. Accudenz is a non-ionic, biologically inert density gradient component. The mixture was transferred to an ultra-clear centrifuge tube (Beckman Coulter, Fullerton, CA, USA), successively overlaid with 350 µl of 30% (w/v) Accudenz in the same buffer and with 100 µl of 25 mM HEPES, pH 7.5, containing 100 mM NaCl. The mixture was centrifuged at 100,000xg for 4 hours at 4°C in the L-80 XP ultra-centrifuge

using a SW55Ti rotor (Beckman Coulter). After ultra-centrifugation, 60 μ l fractions were sequentially collected from the top of the gradient and examined by SDS-PAGE (sodium dodecyl sulphate-polyacrylamide gel electrophoresis) and Western immuno-blot analyses as described below.

Purification of CrdS through Immobilized Metal Affinity Chromatography (IMAC)

The CrdS protein synthesised in the presence of Brij-58 in dialysis mode was equilibrated in 10 mM $\text{Na}_2\text{HPO}_4 \cdot 2\text{H}_2\text{O}$, 150 mM NaCl and 10 mM imidazole, pH 8.0, and added to the Ni-NTA resin (Bio-Rad, Hercules, CA, USA) pre-equilibrated in the same buffer. The mixture was incubated for 16 hours at 4°C and loaded onto a 1x10 cm Econo-column (Bio-Rad). The flow-through was collected and the resin was washed four times with five bed volumes of a wash buffer (20 mM $\text{Na}_2\text{HPO}_4 \cdot 2\text{H}_2\text{O}$, 300 mM NaCl, 20 mM imidazole, pH 8.0) containing 0.04% (w/v) Brij-58. The CrdS protein was eluted six times with one bed volume of the buffer specified above that contained 50 mM, 100 mM, 150 mM, 200 mM, 250 mM and 500 mM imidazole. The fractions were evaluated by SDS-PAGE and Western immuno-blot analyses using either a mouse IgG2a isotype anti 6xHis monoclonal antibody from Clontech (Takara Bio, Shiga, Japan) or rabbit polyclonal antibody, raised against the intracellular catalytic region of CrdS [2]. The purity of CrdS after IMAC was estimated comparatively based on relative contributions of CrdS and other protein components that were detected on the SDS-PAGE gels.

Preparation of CrdS nanodiscs

Nanodiscs were prepared [23,24] with modifications as described below. The CrdS protein was purified by IMAC as described above, and concentrated in a Microcon Ultracel YM10

microconcentrator, molecular mass cut-off 10 kDa (Millipore Billerica, USA). Approximate protein concentration of CrdS was calculated using a Qubit Protein assay kit (Invitrogen) and SDS-PAGE. The lipid components of nanodiscs comprised either the *E. coli* total lipid extract or POPC (Avanti Polar Lipids, Alabaster, AL, USA) that were prepared essentially as described for liposomes, except that sodium cholate (Sigma) was added to the lipid re-hydration buffer such that the final concentration during reconstitution was between 20-40 mM. The plasmid encoding MSP1E3D1, acquired from Addgene (Cambridge, MA, USA) was prepared as described [28,29]. Empty POPC nanodiscs were prepared at a reconstitution ratio of 130:1 (lipid:MSP), while the nanodiscs containing CrdS were prepared at the 0.5:120:1 (CrdS:lipid:MSP) ratio in a total volume of 225 μ l. The solubilised components were mixed and incubated under rotation for 2 hours at 4°C. Biobeads SM-2 (Bio-Rad) were added to the mixture at 0.5 g/ml to facilitate surfactant removal and to initiate nanodisc assembly. After 16 h, a hole was pierced at the bottom of the test tube using a 0.4 mm needle and the nanodiscs were collected by centrifugation (1,500xg, 2 min, 22°C) into a new test tube. Nanodisc samples were re-centrifuged (10,000xg, 2 min, 22°C) to remove precipitates before SEC. The presence of CrdS protein in nanodiscs was examined by SDS-PAGE and Western immuno-blot analyses on a polyvinylidene difluoride (PVDF) membrane with detection using a mouse 6xHis monoclonal antibody (Clontech).

Purification of the CrdS nanodiscs through SEM - The CrdS nanodiscs were purified at room temperature on a Superdex 200 10/300 GL column (GE Healthcare, Piscataway, NJ, USA) connected to an ÄKTA™ Purifier UPC-10 system (GE Healthcare). The void volume of the Superdex column (8 ml) was determined with Blue Dextran. After pre-equilibration of the column in TBS buffer (40 mM Tris, 0.3 M NaCl, pH 7.4), samples (225 μ l) were pre-filtered through 0.45 μ m nylon ISO-Disc filters (Supelco, Bellefonte, PA, USA) and run at a flow rate of 0.5 ml/min in TBS on the ÄKTA™ Purifier. Peaks were monitored at 254 nm and 1 ml fractions were collected.

The nanodisc samples were concentrated in a Microcon Ultracel YM10 micro-concentrator to approximately 200 μ l volumes and kept at 4°C until analysis.

Analysis of CrdS nanodiscs by small-angle X-ray scattering using synchrotron radiation

Small-angle X-ray scattering (SAXS) data of CrdS nanodiscs were collected on the SAXS/WAXS beamline of the Australian Synchrotron (Melbourne, Australia) using a Pilatus-1M pixel-array detector (Dectris, Switzerland). For each data set 25 frames of a 2-second exposure time were collected from a sample moving through the X-ray beam at a constant 5 μ l/s flow rate in a temperature-controlled 1.5 mm quartz capillary. Solutions of CrdS inserted in the *E. coli* total lipid extract or POPC nanodiscs were measured at 30°C in TBS buffer at a single MSP-based protein concentration (~0.1 mg/ml). The sample-to-detector distance was 1.6 m, covering a range of momentum transfer $0.01 \text{ \AA}^{-1} < q < 0.6 \text{ \AA}^{-1}$ ($q = 4\pi\sin\theta/\lambda$, where 2θ is the scattering angle and $\lambda = 1.03 \text{ \AA}$ is the X-ray wavelength). Comparison of successive 2-second frames revealed no detectable radiation damage. Data from the detector were normalized to the transmitted beam intensity, averaged and scattering of the buffer solutions was subtracted using the ScatterBrain software package available at the Australian Synchrotron. The SAXS profiles were analysed using the latest cross-platform ATSAS package [30] and scattering density distributions were determined by indirect Fourier transformation (IFT) using the program GNOM [31].

SDS-PAGE, Western immuno-blot analyses and protein determination

Typically, 5 μ l of CF reactions was evaluated by SDS-PAGE analysis as described [2], except that prior to loading on SDS-PAGE gels, the protein samples were incubated for 30 min at 37°C in the SDS-PAGE loading buffer. The proteins contained in CF reactions included newly synthesised

CrdS and wheat germ extract components. The overall protein concentration varied between 5-6 mg per ml. The Western immuno-blot analysis [2] was carried out with 0.45 μ m PVDF transfer membranes (Amersham Biosciences, Little Chalfont, Buckinghamshire, UK). Working dilutions of antibodies were as follows: anti His 1:4000 (v/v), anti CrdS 1:4000 (v/v) and secondary antibody 1:5000 (v/v). Working solutions of antibodies were prepared in 25 mM Tris-HCl buffer, pH 7.5 containing 137 mM NaCl, 3 mM KCl and 0.05% (w/v) Tween 20. Blots were incubated with antibodies for a duration between one to 16 hours with gentle agitation at 4-8°C. The blots were developed with the Novex® ECL HRP Chemi-Luminescent substrate Reagent Kit (Invitrogen) or with the BCIP/NBT-purple liquid reagent (Sigma) according to the manufacturer's instructions and the images were scanned (Clix Science Instruments, Shanghai, China). Where Transcend tRNA was used, immuno-blot detection was carried out *via* streptavidin conjugated with the alkaline phosphatase chromogen (Sigma) and the membranes were developed with the BCIP/NBT-purple liquid reagent until a desired intensity was achieved. Protein staining on SDS-PAGE gels proceeded either by Coomassie Brilliant Blue R-250 (Sigma) [2] or through SilverQuest Silver Staining Kit (Invitrogen). Total protein staining on PVDF membranes proceeded with Ponceau S (Sigma). Protein concentration was determined using the Qubit Protein Assay Kit (Invitrogen) or by the Protein Assay Kit, based on a Coomassie Brilliant Blue G-250 dye shift (Bio-Rad) [2]. Precision Plus protein molecular mass standards were from Bio-Rad. Purity of CrdS preparations resolved by IMAC and density gradient centrifugation was determined visually based on relative contributions of individual protein bands on SDS-PAGE gels. Semi-quantitative estimation of protein content on SAS-PAGE gels was based on known amounts of BSA.

Other procedures

Tryptic mapping of CrdS by Matrix-Assisted Laser Desorption Ionization-Time of Flight Mass Spectrometry - The band corresponding to synthesized CrdS with Brij-58 in dialysis mode, was excised from the SDS-PAGE gel and placed in sterile Milli-Q water. The protein was digested with trypsin and the peptide mixture was analysed *via* MALDI-TOF/TOF MS. The MS and corresponding MS/MS spectra were combined and submitted to a Mascot database search as described [2].

CrdS proteo-liposomal particle sizing - CrdS proteo-liposomes (250 µl of fraction 3 following the Accudenz density ultra-centrifugation) and empty liposomes were centrifuged (10,000xg, 2 min, 22°C), the pellet was re-suspended in 50 mM MOPS-KOH buffer, pH 7.8 to a volume of 150 µl and dialysed in the D-Tube™ Dialyzer Mini tubes (Novagen, Madison, WI, USA) for 16 hours at 4°C against the same buffer to remove Accudenz. The dialysed, non-concentrated proteo-liposomes (50 µl) were mixed with 950 µl of the 50 mM MOPS-KOH buffer, pH 7.8. The diameter of the liposomes was determined using dynamic light scattering with the NICOMP 380 Particle Sizing Systems (Santa Barbara, CA, USA) operating in vesicle mode and the data was weighted on a number of liposomes.

Liposome-associated topology of CrdS - CrdS (60 µg) in the DMPC liposomes was digested in 50 mM Tris-HCl, pH 8.0, 0.5 mM EDTA and 1 mM DTT with the TEV protease (2 µg) at room temperature for 24 hours. The TEV protease was prepared in-house using the pRK793 expression plasmid [32]. Topology of CrdS was analysed through Western immuno-blot analysis with anti 6xHis antibody (Clontech) as described above.

Transmission electron microscopy (TEM) of liposomes and CrdS nanodiscs - CrdS-occupied and empty DMPC liposomes were purified through floatation in an Accudenz density gradient as described above. About 20 µl of the purified, non-concentrated specimen of liposomes from fraction 3 was placed on a thin piece of parafilm. The carbon coated grid was floated on the droplet for 10 minutes to let liposomes absorb. The grids were washed thrice with 50 mM HEPES, pH 7.5

containing 100 mM NaCl, followed by sterile Milli-Q water and air dried. The grids were stained with aqueous 0.5% (w/v) uranyl acetate (Sigma) and washed five times with water and air dried. For nanodiscs, both empty and CrdS-assembled discs were imaged *prior* to purification through SEC. Crude nanodiscs were absorbed for one minute onto collodion and carbon coated nickel grids that were washed as described above, stained with aqueous 2% (w/v) uranyl acetate and processed as specified for liposomes. The liposomes and nanodiscs were imaged on the transmission electron microscope Philips CM 100 (FEI, Hillsboro, Oregon, USA) operated at 80 kV, at the Adelaide Microscopy Centre of the University of Adelaide.

(1,3)-β-D-Glucan synthase activity - The reaction mixtures contained 3.4 mM UDP-[³H]-glucose (specific activity 10-45 Ci/mmol) (Perkin Elmer, Waltham, MA, USA), 80 μg α-amylase, 0.27 mM GTP, 9 mM MgCl₂ (all from Sigma), 2.2 mM laminaribiose (Megazyme, Bray, Wicklow, Ireland) and 10 μl of enzyme samples [33,34]. The enzyme samples were taken from CF reactions and represented either non-concentrated CrdS synthesised with Brij-58 or Ac-AAAAAAD, and CrdS co-translationally inserted in the *E. coli* total lipid extract liposomes. The enzyme activities of CrdS reconstituted in the *E. coli* total lipid extract or POPC nanodiscs were also measured. The mixed membrane fraction isolated from *S. cerevisiae*, as described below, was used as a positive control for activity measurements [33,34]. The (1,3)-β-D-glucan synthase reactions incubated at 25°C for various time intervals were stopped by adding 50 μl of 10% (w/v) trichloroacetic acid and the mixtures were filtered using the Millipore filter method [34]. The radioactivity incorporated into (1,3)-β-D-glucan, which represents the product of the synthetic reaction, was measured by scintillation counting using the EcoLite scintillant (MP Biomedicals) and a LS6500 Scintillation Counter (Beckman Coulter).

The mixed membrane fraction of *S. cerevisiae* was prepared from cells grown in the YPD (yeast extract-peptone-dextrose) medium at 28°C. The cells were harvested in the early logarithmic phase

of growth. Cell pellets were resuspended in buffer A [25 mM HEPES pH 7.8, 5 mM EDTA, 10 mM NaF, 1 mM phenylmethylsulphonyl fluoride, 1 mM DTT, EDTA-free Complete Protease Inhibitors and 30% (v/v) glycerol] and disrupted with glass beads (Sigma) in a Bead-Beater (Biospec Products, Bartlesville, OK, USA). The disintegrated cells were centrifuged (12,000xg, 10 min, 4°C), the pellet was re-suspended in buffer A, transferred to the Polyallomer centrifuge tubes (Beckman Instruments, Fullerton, CA, USA) and centrifuged (100,000xg, 50 min, 4°C). The resulting pellet was resuspended in buffer A with 2 μ M GTP and 5 mM UDP-glucose, and stored at -80°C in aliquots. The (1,3)- β -D-glucan product was characterised as described [34]. Here, the radioactive product was hydrolysed by (1,3)- β -D-exo-glucanase from Mollusc (Sigma) for 16 hours at 30°C and remaining radioactivity was measured by scintillation counting as described above. Treatments of radioactive products by boiled (1,3)- β -D-exo-glucanase and α -amylase (Sigma) were conducted for 16 hours at 30°C and remaining radioactivity was estimated.

Results

Construction of pEU-EO1TM expression plasmids for wheat germ cell-free protein synthesis

PCR-amplified full-length cDNA of CrdS was cloned into the pGEM-T Easy vector system, using the primers listed in Table 1. The amplified CrdS coding regions inserted in the pGEM-T-CrdS plasmids were sequenced and found to be correct. The *Xho*I- and *Not*I-digested blunt-ended pGEM-T-CrdS DNA fusions were sub-cloned in-frame into the pEU-EO1TM vectors affording the three expression plasmids pEU-EO1-His-CrdS, pEU-EO1-His-Xa-CrdS and pEU-EO1-His-TEV-CrdS. These DNA fusions contained the coding region of CrdS and the sequences encoding 6xHis affinity tags and either Factor Xa or TEV (Tobacco Etch Virus) proteolytic sites at their 5'-termini, followed with cloning overhang sequences of 9-12 bp long. The 6xHis tag and the TEV site in the

pEU-EO1-His-TEV-CrdS plasmid were separated by a 7-residue linker DYDIPTT that was designed to facilitate cleavage of a 6xHis affinity tag *via* the TEV protease. The cleavage of 6xHis-TEV-CrdS with the latter protease would leave an additional Gly residue at the NH₂-terminus of CrdS, while the cleavage with the Factor Xa protease afforded an intact NH₂-terminus of CrdS.

CrdS is synthesised during wheat germ cell-free protein synthesis in bilayer mode and co-translationally inserted in liposomes

Efficiency of wheat germ CF protein synthesis (WG-CFPS) system was investigated in bilayer mode adopting de-coupled transcription and translation reaction modes. The translation was carried out for 16 hours at 20°C in the presence of DMPC liposomes with all three pEU-EO1-His-CrdS, pEU-EO1-His-Xa-CrdS and pEU-EO1-His-TEV-CrdS mRNAs. As indicated in Fig. 1, with all three DNA fusions, SDS-PAGE profiles showed good yield of CrdS in the presence of DMPC liposomes. Here, low µg quantities of CrdS per 150 µl of reaction mixtures were obtained (Fig. 1, lanes 1-3), while no CrdS was synthesised in the reaction mixture lacking mRNA (Fig. 1, lane 4). We observed a discrepancy between migration of the synthesised 6xHis-CrdS, 6xHis-Xa-CrdS and 6xHis-TEV-CrdS proteins on the SDS-PAGE gels and their theoretical molecular masses, however this anomaly was not unprecedented [35].

The data presented in Fig. 1 (lane 3) with the His-TEV-CrdS construct was corroborated in a separate experiment (Fig. 2). The identity of the synthesised CrdS protein was verified through Western blot using the anti-CrdS antibody (Fig. 2B, lanes 1 and 2). In addition, synthesis of CrdS was also confirmed by detection with alkaline phosphatase-conjugated streptavidin (Fig. 2C, lanes 1 and 2). Our next task was to assess, if synthesised CrdS was co-translationally inserted in the DMPC liposomes or if CrdS aggregated during translation (Fig. 2). When the translation reaction

with CrdS was separated into the supernatant and pellet fractions by centrifugation, the synthesised CrdS protein remained associated with the pellet fraction while hardly any CrdS protein was detected in the supernatant, pointing to the fact that CrdS may have been successfully reconstituted in DMPC liposomes (Fig. 2C and Fig. 3). As indicated in Fig. 2B, CrdS could efficiently be detected with the rabbit polyclonal antibody, raised against the intracellular catalytic region of CrdS [2], or with the streptavidin-alkaline phosphatase conjugate (Fig. 2C). In the latter case, streptavidin targets biotinylated lysine residues that had been incorporated into CrdS during CFPS from biotinylated tRNA. Hence, this assay allows for detection of only newly synthesised CrdS protein molecules from CrdS mRNA. It is of note that the higher molecular mass protein bands that migrated between 70 and 250 kDa (Fig. 2C) resulted from the detection of native biotinylated proteins contained in the wheat germ extract, and not due to oligomeric assemblies of CrdS. Notably, the protein of about 130 kDa size found in all preparations (Fig. 2B) most likely represented a wheat germ protein as it was not detected *via* alkaline phosphatase-conjugated streptavidin (Fig 2C).

To confirm that the pellet fraction contained the CrdS DMPC-liposomes and not simply aggregated CrdS, the proteo-liposomes of approximately 100 nm diameter were subjected to floatation by Accudenz density gradient ultra-centrifugation and then detected [36]. As indicated in Fig. 3 (lane 3), fractions with the CrdS proteo-liposomes detected with anti-CrdS antibody, floated near the top of the gradient. This observation highlighted the fact that over 95% of CrdS was successfully inserted co-translationally in the DMPC liposomes, while only very low amount of synthesised CrdS was found at the bottom of the test tube in the form of an aggregate (Fig. 3 inset, lane 10). Further, the floatation through Accudenz density gradient using ultra-centrifugation substantially improved the purity of the CrdS proteo-liposomes. The purified CrdS-liposomal preparations (Fig. 4A) and those without CrdS (empty DMPC liposomes) were imaged by transmission electron

microscopy (TEM). In these images (Fig. 4), the proteo-liposomes with or without CrdS appeared as rounded objects, sizes of which ranged between 80 and 100 nm. No significant variations in the appearance of liposomes with and without reconstituted CrdS were observed (Figs. 4A and 4B). Notably, in both cases fusion of uni-lamellar liposomes into the multi-lamellar structures was observed.

Screening of CrdS production using wheat germ cell-free protein synthesis in bilayer mode with liposomes prepared from a variety of lipids

The next question to address was whether other types of lipids could also lead to successful incorporation of CrdS in their bilayers. We investigated effects of lipids on CrdS synthesis in the high-throughput bilayer mode. Here, CrdS was synthesized in the presence of a variety of liposomes, prepared from a single zwitterionic, anionic and cationic lipid components or a mixture of lipids at concentrations ranging from 2.5 mg/ml to 10 mg/ml (Table 3). The CrdS protein synthesised under these conditions was detected directly on SDS-PAGE gels, as described in the Materials and methods section. The yields of CrdS synthesised in the presence of liposomes prepared from a variety of lipids are summarised in Fig. 5. The highest yields of CrdS occurred with liposomes prepared from zwitterionic lipids DMPC and with liposomes prepared from soybean asolectin and *E. coli* lipids, followed by liposomes prepared from zwitterionic DOPC and POPC (Fig. 5). No CrdS was synthesised in the presence of liposomes prepared from charged lipids, *i.e.* DOPG (anionic lipid) and DOTAP (cationic lipid). However surprisingly, when the liposomes were prepared from DOPG (anionic lipid) and POPE (zwitterionic lipid) in a ratio of 2:3 by weight, the CrdS protein was synthesised (Fig. 5). The liposomes prepared from the total lipid extract of *E. coli* also led to high yield of CrdS; this yield was comparable to that during CFPS with the zwitterionic DMPC and with the asolectin liposomes. The conclusion from these experiments was that lipid type

and composition were of paramount importance for a successful co-translational insertion of CrdS in high yields.

CrdS production through wheat germ cell-free protein synthesis in bilayer mode with surfactants, surfactant peptides and amphipols

A range of surfactants, surfactant peptides and amphipols were screened during CFPS of CrdS (Table 2, Figs. 6 and 7). The list of surfactants, their sources and concentrations that were above their CMC are summarized in Table 2. The effect of the tested surfactants on synthesis of CrdS was variable (Fig. 6). Out of nine surfactants tested (Table 2), four surfactants namely Brij-58, digitonin, Triton X-100 and Tween 80 were compatible with CFPS, leading to production of CrdS in a soluble form, while with β -OG, NP40 and CHAPS the CrdS synthesis was not observed (data not shown). The highest yields of CrdS were achieved with Brij-58, followed by digitonin, Triton X-100 and Tween 80 (Fig. 6).

CFPS of CrdS in the presence of the three acetylated surfactant peptides Ac-AAAAAAD (Ac-Ala-Ala-Ala-Ala-Ala-Asp), Ac-IIID (Ac-Ile-Ile-Ile-Asp), Ac-LLLK-NH₂ (Ac-Leu-Leu-Leu-Lys-NH₂) was carried out at 1 mM, 2 mM and 4 mM concentrations (Fig. 7). The CrdS protein was synthesised in the presence of all the three peptides, although the yields of CrdS varied. CrdS yield was higher in the presence of Ac-AAAAAAD and Ac-IIID at 1 mM and 2 mM concentrations (Fig. 7, lanes 3-4 and 6-7), compared to that with Ac-LLLK-NH₂ (Fig. 7, lanes 9-10). Notably, at 4 mM concentrations of the surfactant peptides, CrdS synthesis was either decreased or inhibited, in particular with Ac-AAAAAAD (Fig. 7, lanes 5, 8 and 11).

Finally, the presence of amphipols A8-35 and SMA in 0.5% (w/v) to 4% (w/v) concentrations was found to be inhibitory during CFPS of CrdS (data not shown).

Synthesis of CrdS with Brij-58 in dialysis mode and purification of CrdS through Immobilized Metal Affinity Chromatography

Optimal conditions for WG-CFPS of CrdS in bilayer mode were selected to set up a reaction in dialysis mode, as described in the Materials and methods section. The synthesis was carried out in the presence of 0.04% (w/v) Brij-58 for 24 hours, 48 hours and 72 hours, and the reaction mixtures were analysed by SDS-PAGE (Fig. 8, lanes 1-3). Based on our semi-quantitative estimations, yield of CrdS in the presence of Brij-58 was as high as 1 mg/ml after 48 hours (Fig. 8, lane 2) and this yield remained unchanged after the next 24-hour incubation period (Fig. 8, lane 3).

The CrdS protein synthesized through dialysis mode in the presence of Brij-58 was purified by Immobilized Metal Affinity Chromatography (IMAC) using a Ni-NTA affinity resin. The data in Fig. 9 indicate that CrdS could be purified significantly from a crude translation reaction by IMAC, and that reasonable purity of CrdS was achieved in the fractions eluted with 150 mM, 200 mM, 250 mM imidazole (Fig. 9, lanes 9-11). On the other hand, contaminating components were removed during the 20 mM imidazole washing steps (Fig. 9, lanes 3-6). The protein sample eluted with 250 mM imidazole contained the highest amount of CrdS with fewer contaminants as detected on the Coomassie Brilliant Blue R-250-stained SDS-PAGE gel (Fig. 9, lane 11, black arrow). The purity of CrdS (Fig. 9, lane 11), which should be the only newly synthesised membrane protein in this preparation, was estimated to be between 50% and 60%. This estimation formed a basis for stoichiometry to assemble CrdS nanodiscs.

CrdS synthesised through wheat germ cell-free synthesis is a full-length protein

CrdS synthesized in the presence of Brij-58 in dialysis mode was purified by IMAC, and analysed by SDS-PAGE and the Western immuno-blot analysis using the anti 6xHis antibody and the rabbit polyclonal antibody, raised against the intracellular CM of CrdS [2]. The protein band corresponding to CrdS was excised from the SDS-PAGE gel and subjected to tryptic digestion. The analysis of tryptic fragments was performed by MALDI-TOF/TOF MS (Table 4). A Mascot database searches of the peptide sequences matched perfectly the generated peptide ions to the putative (1,3)- β -D-glucan synthase catalytic subunit (GenBank accession AF057142) (Table 4).

Reconstitution of CrdS in nanodiscs and purification through SEC

The CrdS protein synthesised in the presence of Brij-58 and purified by IMAC as described above, was reconstituted in the *E. coli* total lipid extract or POPC nanodiscs (Fig. 10). Here, the CrdS:lipid:MSP components were mixed in a 0.5:120:1 molar ratio and following surfactant removal, the self-assembled nanodiscs were purified by SEC on the Superdex 200 column. As indicated in Fig. 10A, both types of CrdS nanodiscs eluted at significantly faster rates (*cf.* black and dotted traces in Fig. 10A) than the empty POPC nanodiscs (*cf.* dotted line in Fig. 10A), while the remaining MSP protein and other contaminant proteins eluted later (18-23 ml) (Fig. 10A).

To confirm that the CrdS protein successfully reconstituted in the *E. coli* total lipid extract and POPC nanodiscs, the fractions from SEC that eluted between 6 and 9 ml (Fig. 10A) were pooled, concentrated and examined by silver-stained SDS-PAGE (Fig. 10B) coupled with a Western immuno-blot analysis on PVDF membranes (Fig. 10C). As documented in Figs. 10B and 10C (lanes 2 and 3), the CrdS protein could successfully be detected using both analytical approaches.

Notably, the Western immuno-blot analysis operated within a detection limit (Fig. 10C, lanes 2 and 3) using the mouse anti 6xHis monoclonal antibody. This observation suggested that 6xHis tag could be partly obscured after CrdS is reconstituted in nanodiscs. We could also observe that the CrdS proteins reconstituted in the *E. coli* lipids or POPC nanodiscs migrated on the SDS-PAGE gel in a form of diffused bands. These protein bands, which are delineated by two arrowheads (Figs. 10B, and 10C, lanes 2 and 3) migrated slightly slower than CrdS purified by IMAC (Fig. 10C, lane 1, white arrow). We suggest that these differences in CrdS migration could result from a tight association of CrdS with lipids. Contrary to these specific associations of CrdS with the *E. coli* or POPC lipids, purified CrdS migrated in a form of a sharp protein band in the absence of lipids (Fig. 10C, white arrow). To determine morphological properties of CrdS nanodiscs, they were imaged by TEM prior to SEC. The TEM images of CrdS nanodiscs made from *E. coli* lipids (Fig. 10D, top panel) and POPC (Fig. 10D, bottom panel), indicated that these nanoparticles appeared poly-disperse in nature (Fig. 10D). Although substantial proportions of both types of the CrdS nanodiscs were non-clustered, clumps of nanodiscs were observed (Fig. 10D; white and black arrows in top and bottom panels).

Characterisation of CrdS nanodiscs by small-angle X-ray scattering using synchrotron radiation

To find out if the SEC-purified CrdS nanodiscs were formed correctly as the bilayer-embedded membrane protein complexes, the purified CrdS nanodiscs were characterised by SAXS (Fig. 11). The SAXS profiles of CrdS reconstituted in the *E. coli* total lipid extract or POPC nanodiscs were typical of those reported for other membrane-inserted proteins in nanodisc bilayer environments. These nanodiscs typically have a characteristic broad maximum at $\sim 0.1 \text{ \AA}$ that corresponds to the phospholipid bilayer [37,38]. Using an indirect Fourier transformation (IFT) approach [31,39], the

scattering density distributions of the protein-lipid complexes were determined (Fig. 11, inset) that provided a real-space representation of the scattering data. The distributions for both CrdS nanodiscs showed alternating positive and negative peaks at short distances ($<50 \text{ \AA}$), reflecting the complex contrast landscape across the bilayer resulting from the lower scattering length density of the inner alkyl layer relative to solvent (TBS buffer). An extended tail of positive scattering density was observed with the maximum particle diameter (D_{max}) approaching $\sim 175 \text{ \AA}$ for both CrdS nanodiscs, indicating that solvent-exposed CrdS extended into solution away from the membrane. These quantitative particle diameter data of both types of CrdS nanodiscs agreed well with those obtained through TEM imaging (*cf.* Fig. 10D and Fig. 11). The scattering density distributions suggested that an approximate bilayer width of the purified CrdS nanodiscs was 50 \AA . Again, the latter parameter was consistent with the distributions reported in the literature [37,38,40].

CrdS synthesised with the surfactant peptide Ac-AAAAAAD or reconstituted in the *E. coli* liposomes exhibits (1,3)- β -D-glucan synthase activity

The CrdS enzyme is believed to operate as the UDP-glucose: (1,3)- β -D-glucan 3- β -D-glucosyltransferase (EC 2.4.1.34). Thus, to find out if CrdS was synthesised in a catalytically active form, (1,3)- β -D-glucan synthase activity assays were carried out. This assay directly evaluates synthesis of the (1,3)- β -D-glucan product, where the formed radioactive product is collected by filtration on millipore filters and its radioactivity is evaluated by scintillation counting [34]. Because high yields of the CrdS protein were required for these enzyme activity measurements, CrdS was synthesised in the presence of the surfactant Brij-58 and the surfactant peptide Ac-AAAAAAD, or co-translationally inserted in the *E. coli* total lipid extract liposomes, in dialysis mode. A mixed membrane fraction isolated from *S. cerevisiae* and containing a membrane-associated (1,3)- β -D-

glucan synthase [33,34], served as a positive control for these (1,3)- β -D-glucan synthase activity measurements.

The data in Table 5 indicated that CrdS synthesised in the presence of Brij-58 was not active, as there was no increase in radioactivity of the (1,3)- β -D-glucan product synthesised from UDP-[3 H]-glucose serving as a donor substrate. Similarly, CrdS that was reconstituted in *E. coli* total lipid extract or POPC nanodiscs was found to be catalytically incompetent (Table 5). Conversely, the CrdS proteins synthesised with the surfactant peptide Ac-AAAAAAD or co-translationally inserted in the *E. coli* liposomes, were active (Table 5). The average specific activities, calculated from two independent measurements, were 0.18 mU/mg and 0.22 mU/mg of protein for CrdS synthesised with Ac-AAAAAAD or for CrdS co-translationally inserted in the *E. coli* liposomes, respectively (Table 5). In comparison, the specific activity of (1,3)- β -D-glucan synthase isolated from the *S. cerevisiae* membranes was 1.97 mU/mg protein (Table 5). The latter value was nearly ten fold higher than the specific activities of CF-synthesised CrdS, which was not surprising as the native mixed membrane fractions of *S. cerevisiae* were used for activity measurements.

Discussion

Membrane proteins are fundamental to essential cellular functions, yet information on their structural and functional properties is limited. At the end of August 2012, around 355 unique 3D structures of membrane monotopic and polytopic β -barrel and α -helical proteins have been deposited in databases (<http://blanco.biomol.uci.edu/mpstruc/>) compared to nearly 84,000 released structures of soluble proteins. The reasons for this low incidence of 3D membrane protein structures compared to those of soluble proteins are manifold. For example, membrane proteins exist in low abundance and a variety of conceptual difficulties associated with their production and isolation

remain unresolved. Although, relatively simple cloning of membrane proteins' cDNA into a diversity of vector systems is prevalent [41-45], membrane proteins' production, purification and crystallisation are less successful and require extensive effort. To this end, the majority of 3D structures of resolved membrane proteins were produced in bacterial hosts, and fewer of them have been obtained in yeast, insect, mammalian cells or through CFPS [10,11].

CFPS systems are an alternative to cell-based systems, the popularity of which started growing only recently with the advent of robotised synthesisers and other technical and conceptual advances [21,22]. An advantage of CFPS is that they allow preparing membrane proteins without residual lipids that are typically co-extracted from membranes and thus researchers can control the lipid composition and environment of synthesised membrane proteins. It has been suggested that the lipid environment around proteins in membranes is responsible for functional modulation of membrane proteins. One of the main CFPS platforms currently used is an eukaryotic wheat germ extract CFPS platform [10-14,17-22], which has been applied in the current work. It has been well documented that WG-CFPS systems enable rapid production of proteins and thus this platform plays an important role in modern functional genomics [10,11,17-22]. This system holds promise in particular for eukaryotic membrane proteins [10,11], as they almost always require post-translational modifications that can be achieved *via* coupling of CFPS systems with *in-situ* glycosylation, phosphorylation, *etc.*

In the current work, our target CrdS transferase enzyme is confined within cell membranes of *Agrobacterium* sp. [2]. This enzyme is believed to catalyse formation of a (1,3)- β -D-glucan (curdlan) polymer by a repetitive addition of glucosyl residues from the UDP-glucose donor substrate. CrdS as a GT2 family glycosyl transferase enzyme (CAZy database) is clustered with other plant membrane enzymes of paramount significance, such as cellulose, (1,3)- β -D-glucan and

(1,3;1,4)- β -D-glucan synthases [2-4]. The CrdS protein harbours seven membrane spanning α -helices, contains a single CM and has a predicted N_{out}-C_{in} topology [2]. Only a few 3D structures of the GT2 enzymes were elucidated up to date, notably all of them by X-ray crystallography [5-7, Polani, Kumaran, Burley and Swaminathan, unpublished data]. However, all these enzymes do not harbour membrane α -helices and essentially embody catalytic modules that fold into α/β architectures [5-7, Polani, Kumaran, Burley and Swaminathan, unpublished data]. Thus, an urgency to resolve a 3D structure of a membrane-associated transferase enzyme in the GT2 family remains.

Our previous attempts to obtain sufficient yield of the full-length CrdS protein in the *E. coli* host for 3D structural, biochemical and biophysical analyses failed [2]. In these experiments we used a variety of bacterial vectors (*e.g.* pET15b, pBAD24, ChampionTM, pET SUMOTM), but irrespective of the conditions, the heterologous expression led to production of truncated forms of CrdS that were produced *via* abortive translation. Hence, in our current study we concentrated our efforts on CFPS of full-length CrdS based on a well-defined wheat germ system, which has been documented to produce sufficient amounts of proteins for both analytical and preparative purposes [10,11,46].

When investigating the initial conditions for WG-CFPS of CrdS, we established that the purities of plasmid DNA fusions, expressed as a A₂₆₀/A₂₈₀ ratio for transcription reactions (the suitable range is 1.8-2.0), as well as purities of mRNAs for translation reactions (lack of low molecular mass mRNA species of less than 500 bp) were of paramount importance to detect synthesis of full-length CrdS and obtain good yield. We methodically examined the efficiency of WG-CFPS in bilayer and dialysis modes, using a wide range of surfactants, surfactant peptides and amphipols, and of liposomes prepared from a variety of lipids. We found optimal conditions for excellent yield of CrdS in the presence of surfactants, surfactant peptides, and liposomes. The best performing surfactant was with Brij-58, which is considered to be mild, probably owing to its low CMC [47].

On the other hand, the addition of amphipols A8-35 or SMA inhibited WG-CFPS of CrdS. The reason for this inhibitory behaviour of amphipols is not fully understood and could result from either functional de-stabilisation of ribosomes contained in wheat germ, or that amphipols directly interfere with structure of ribosomes and thus CF synthesis. To this end, it has been suggested that A8-35 and sulfonated amphipols may interact with basic patches at surfaces of ribosomal nanoparticles [48].

The CrdS proteins containing 6xHis affinity tag, or 6xHis affinity tag and Factor Xa or TEV proteolytic sites synthesised in WG-CFPS typically migrated around the ranges of 56-60 kDa, though their calculated masses are between 73-76 kDa. Although unexpected, our observations with this anomalous migration of membrane CrdS were not unprecedented, since it was previously observed that membrane proteins' band positions do not always correlate with their formula molecular masses [35]. Through tryptic mapping and Mascot database searches, we found out that the generated peptide ions in length of 10-32 amino acid residues, matched perfectly to the putative (1,3)- β -D-glucan synthase catalytic subunit (GenBank accession AF057142). Hence, the MALDI-TOF/TOF MS analysis in conjunction with Western immuno-blot detection unambiguously confirmed that full-length CrdS was synthesised through WG-CFPS.

Excellent yield of CrdS in the presence of artificial liposomes prepared from *E. coli* lipid extract were obtained through WG-CFPS. This high yield was not unexpected as CrdS is a membrane protein of a bacterial origin. It has been estimated that the most abundant phospholipid species (70%) in the inner membrane of *E. coli* is POPE [49]. It consequently seemed logical that the addition of POPE to DOPG, by 3:2 weight ratio lead to CrdS synthesis, while DOPG alone did not support synthesis. Surprisingly, when the liposomes prepared from soybean asolectin lipids were added to CFPS translation reactions, high yield of CrdS was also obtained. It is of note that the

soybean (plant) asolectin lipids represent a complex mixture of phospholipids such as lecithin, cephalin and phosphatidylinositol in equal proportions, along with minor amounts of other phospholipids and polar lipids.

To determine the liposome-associated topology of CrdS following co-translational insertion, the CrdS protein was synthesised in the presence of 100 nm DMPC liposomes. We surmised that in these liposomes, CrdS could either adopt $N_{out}-C_{in}$ topology, $N_{in}-C_{out}$ topology or a mixture of both. Here, the $N_{out}-C_{in}$ topology of CrdS was predicted previously through the PRED-TMR algorithm [2,41]. If the $N_{out}-C_{in}$ topology was occurring in the DMPC liposomes, then the NH_2 -terminus of the CrdS protein would protrude to the exterior of the liposomes and CM would localize to the liposomal lumen. To this end, the CrdS proteo-liposomes purified through floatation by Accudenz density gradient ultra-centrifugation, were digested with the TEV protease and analysed through a Western immuno-blot analysis. When the TEV-treated CrdS proteo-liposomes separated by SDS-PAGE were detected with the anti 6xHis antibody, the reactivity of the TEV-treated CrdS towards this antibody was significantly diminished. Further, the protein band of TEV-treated CrdS on the SDS-PAGE gel shifted to a lower molecular mass and became diffuse (data not shown). These observations suggested that in some CrdS molecules, the NH_2 -terminus harbouring the 6xHis tag could have been excised by the TEV protease. Thus, in some DMPC liposomes, the NH_2 -terminus of CrdS was likely pointing to the exterior of the liposomes, while the other liposomal population contained CrdS in the $N_{in}-C_{out}$ topology. Hence, it can be concluded that CrdS reconstituted in the DMPC liposomes exhibited a random orientation. The possible explanation for this random distribution could be in a diameter (100 nm) and hence high-angle curvature of proteo-liposomes. This curvature could hinder proper insertion of large CM of CrdS into the liposomal lumen, whereas larger diameter proteo-liposomes may be conducive to the correct $N_{out}-C_{in}$ topology of CrdS.

Recombinant CrdS synthesised with the Ac-AAAAAAD surfactant peptide or co-translationally inserted in the *E. coli* lipid extract liposomes was found to be active. On the other hand, CrdS synthesised with Brij-58 or reconstituted in the *E. coli* lipids and POPC nanodiscs was inactive. The latter observation indicates that the CrdS protein synthesised with the surfactant Brij-58 may not have been properly folded and also that reconstitution of CrdS in nanodiscs could not restore CrdS's catalytic activity. However, the observation that CrdS synthesised with the surfactant peptide Ac-AAAAAAD was active, may suggest that surfactant peptides could self-assemble to form a belt surrounding membrane proteins leading to formation of a stable surfactant peptide-membrane protein complex [50]. To find out if the radioactive material synthesised by CrdS (and by the mixed membrane fractions of *S. cerevisiae*) produced the (1,3)- β -D-glucan polymer, the radioactive material was hydrolysed by the (1,3)- β -D-exo-glucanase enzyme that is known to hydrolyse (1,3)- β -D-glucan through an exo-hydrolytic mechanism to glucose [33,34]. Gratifyingly, we found that the radioactivity incorporated in the (1,3)- β -D-glucan product had decreased in all cases by approximately 60% by the (1,3)- β -D-exo-glucanase treatment, indicating that a substantial proportion of the material synthesised by CrdS corresponded to the (1,3)- β -D-glucan product. Conversely, the treatment with a boiled (1,3)- β -D-exo-glucanase or α -amylase left the radioactivity incorporated in the (1,3)- β -D-glucan product unchanged, again confirming the chemical identity of the synthesised product.

Reconstitution of membrane proteins in nanodiscs, pioneered by Sligar and co-workers has been described with membrane proteins of various lengths [23,24,51,52]. The advantage of this technique is generation of homogenous nanoscale lipid bilayers, which enclose a desired membrane protein that is exposed to aqueous environments on both sides. These nanodiscs can then be subjected to biophysical, enzymatic and structural investigations. These nanoscale particles can be effortlessly

handled similar to soluble proteins, as their membrane components are shielded by the lipid bilayer milieu, although, specific challenges during nanodiscs construction remain. To this end, the bottleneck represents a gentle isolation or production of a specific membrane protein that can be obtained from biological sources, or expressed and synthesised.

To reconstitute the CrdS protein in nanodiscs, firstly CrdS had to be synthesised in the presence of a mild surfactant Brij-58 in high yield and purified by IMAC. We estimated that nearly 90% of CrdS could be recovered by this purification technique. Subsequently, the surfactant-solubilised CrdS protein was subjected to spontaneous assembly with MSP1E3D1 and either the *E. coli* lipids or a zwitterionic POPC lipid, resulting in spontaneous formation of CrdS:lipid:MSP nanodiscs. The CrdS-containing nanodiscs were then purified by SEC to near homogeneity and both SDS-PAGE and Western immuno-blot analyses indicated the presence of CrdS in these artificial bilayers (Fig. 10). When the CrdS-containing nanodiscs were subjected to SDS-PAGE, the CrdS protein migrated slightly slower than CrdS purified by IMAC, most likely due to associations of CrdS with lipids. These data also indicated that the CrdS protein bound lipid molecules tightly and that the presence of SDS could not entirely abolish these protein-lipid associations. The precise reasons, why CrdS nanodiscs eluted near the void volume during SEC are not known at present. We suggest that at least two factors may play a role. First, CrdS after assembling in nanodiscs could form asymmetrical particles, which are due to the presence of a large catalytic module and a COOH-terminal extension positioned on one side of a nanodisc bilayer, while the other side of a bilayer contains short loops only [2]. Second, CrdS nanodiscs could form clusters of aggregated or stacked particles, formation of which is mediated by Brij-58 that remains tightly associated with the CrdS protein during CFPS, IMAC purification and subsequent nanodisc formation.

The CrdS-loaded nanodiscs purified by SEC were characterised by SAXS. Our experimental SAXS data were found to be consistent with membrane insertion of the CrdS protein into the bilayer of both *E. coli* lipids- and POPC-formed nanodiscs. The SAXS data provided evidence that CrdS nanodiscs have been formed [37,38,40] and gave us confidence to reconstitute CrdS in these bilayers for future, more detailed structural studies. Future work will focus on parameter extraction and modeling from samples at higher concentrations, particularly in the differentiation of empty and CrdS-loaded nanodiscs, and in separation of protein and lipidic scattering *via* contrast variation in small-angle neutron scattering experiments. Future work will also expand upon the initial studies presented in our current work, and explore in-depth bilayer insertion and membrane perturbation caused by CrdS in nanodiscs formed from the *E. coli* lipids and POPC, and from a variety of other lipids.

Finally, meaningful studies of polysaccharide synthases such as CrdS are rare [53] and progress on structural descriptions of β -D-glucan synthases has been slow-moving [3]. This is particularly accurate for synthases of the GT2 family, which contains enzymes required for the synthesis of polysaccharides such as cellulose, (1,3)- and (1,3;1,4)- β -D-glucans [2,3]. It has proved problematic to purify these enzymes from nearly any biological material [2,3], because of a membrane location of these polysaccharide synthases, their low concentration in cellular tissues and a tendency to lose enzyme activity following tissue disruption and isolation. For these reasons, CFPS systems using cDNA fusions offer an alternative route to prepare sufficient amounts of polysaccharide synthases for structural, physicochemical, kinetic and substrate specificity studies.

Conclusions

A set of suitable procedures based on WG-CFPS has been developed leading to high yield of an integral membrane CrdS enzyme from *Agrobacterium* sp. that is classified by the Enzyme Commission as UDP-glucose: (1,3)- β -D-glucan 3- β -D-glucosyltransferase (EC 2.4.1.34). Here, we synthesised full-length CrdS as evidenced by MALDI-TOF/TOF MS, from the pEU-EO1TM plasmids, containing a 6xHis affinity tag and either Factor Xa or TEV proteolytic sites. CFPS afforded good yield of CrdS with a variety of surfactants, surfactant peptides and liposomes through bilayer and dialysis modes. The dialysis mode with the surfactant Brij-58 afforded between 1 and 2 mg per ml quantities of CrdS. IMAC purified CrdS synthesised with Brij-58 was assembled in the *E. coli* lipids or POPC nanodiscs. CrdS synthesised in the presence of the surfactant peptide Ac-AAAAAAD and co-translationally inserted in the *E. coli* liposomes was catalytically competent. We expect that these rapid and efficient WG-CFPS procedures could be used for generation of other membrane catalysts, particularly where large quantities of proteins are required for downstream functional, structural and other applications.

Acknowledgements

We are grateful to Dr Leanne Kelly and Dr Gwenda Mayo (Australian Centre for Plant Functional Genomics) for MALDI-TOF/TOF MS and TEM analyses, respectively. Ramya Sampath is thanked for technical support. Dr Timothy Knowles (University of Birmingham, UK) is acknowledged for providing SMA. Financial support from the Australian Synchrotron Research Program is funded by the Commonwealth of Australia and access to the SAXS/WAXS beamline is also acknowledged.

Funding source

This work was supported by the DP120100900 and LP120100201 grants from the Australian Research Council to MH.

References

- [1] S.J. Stasinopoulos, P.R. Fisher, B.A. Stone, V.A. Stanisich, Detection of two loci involved in (1→3)- β -glucan (curdlan) biosynthesis by *Agrobacterium* sp. ATCC31749, and comparative sequence analysis of the putative curdlan synthase gene, *Glycobiology* 9 (1999) 31-41.
- [2] M. Hrmova, B.A. Stone, G.B. Fincher, High-yield production, refolding and molecular modelling of the catalytic module of (1,3)- β -D-glucan (curdlan) synthase from *Agrobacterium* sp., *Glycoconj. J.* 27 (2010) 461-476.
- [3] B.A. Stone, A.K. Jacobs, M. Hrmova, R.A. Burton, G.B. Fincher, The biosynthesis of plant cell wall and related polysaccharides by enzymes of the GT2 and GT48 families, in: Ulvskov, P. (Ed.), *Plant Polysaccharides Series: Annual Plant Reviews* 41, 109-166, Blackwell Publishing, Danvers, 2011.
- [4] B.L. Cantarel, P.M. Coutinho, C. Rancurel, T. Bernard, V. Lombard, B. Henrissat, The Carbohydrate-Active EnZymes database (CAZy): an expert resource for glycogenomics, *Nucleic Acids Res.* 37 (2009) D233-D238.
- [5] S.J. Charnock, G.J. Davies, Structure of the nucleotide-diphospho-sugar transferase, SpsA from *Bacillus subtilis*, in native and nucleotide-complexed forms, *Biochemistry* 18 (1999) 6380-6385.
- [6] T. Osawa, N. Sugiura, H. Shimada, R. Hirooka, A. Tsuji, T. Shirakawa, K. Fukuyama, M. Kimura, K. Kimata, Y. Kakuta, Crystal structure of chondroitin polymerase from *Escherichia coli* K4, *Biochem. Biophys. Res. Commun.* 378 (2009) 10-14.
- [7] A.L. Lovering, L.Y. Lin, E.W. Sewell, T. Spreter, E.D. Brown, N.C. Strynadka, Structure of the bacterial teichoic acid polymerase TagF provides insights into membrane association and catalysis, *Nat. Struct. Mol. Biol.* 17 (2010) 582-589.

- [8] E.J. Stewart, F. Aslund, J. Beckwith, Disulfide bond formation in the *Escherichia coli* cytoplasm: an *in vivo* role reversal for the thioredoxins, *EMBO J.* 17 (1998) 5543-5550.
- [9] Y. Tsunoda, N. Sakai, K. Kikuchi, Improving expression and solubility of rice proteins produced as fusion proteins in *Escherichia coli*, *Prot. Express. Purif.* 42 (2005) 268-277.
- [10] A.S. Spirin, J.R. Swartz, *Cell-Free Protein Synthesis. Methods and Protocols*, Wiley-VCH Verlag, Weinheim, 2008.
- [11] N. Farrokhi, M. Hrmova, R.A. Burton, G.B. Fincher, Heterologous and cell free expression systems, in: D. Somers, P. Langridge, P. Gustafson (Eds.), *Plant Genomics*, Humana Press Inc., Totowa, *Meth. Mol. Biol.* 513 (2009) 175-198.
- [12] F. Katzen, G. Chang, W. Kudlicki, The past, present and future of cell-free protein synthesis, *Trends Biotech.* 23 (2005) 150-156.
- [13] S. Wagner, M.L. Bader, D. Drew, J.-W. de Gier, Rationalizing membrane protein overexpression, *Trends Biotech.* 24 (2006) 364-371.
- [14] L. Liguori, B. Marques, A. Villegas-Mendez, R. Rothe, J.L. Lenormand, Production of membrane proteins using cell-free expression systems, *Expert Rev. Proteomics* 4 (2007) 79-90.
- [15] D.F. Savage, C.L. Anderson, Y. Robles-Colmenares, Z.E. Newby, R.M. Stroud, Cell-free complements *in vivo* expression of the *E. coli* membrane proteome, *Prot. Sci.* 16 (2007) 966-976.
- [16] D. Schwarz, V. Dötsch, F. Bernhard, Production of membrane proteins using cell-free expression systems, *Proteomics* 8 (2008) 3933-3946.
- [17] F. Junge, S. Haberstock, C. Roos, S. Stefer, D. Proverbio, V. Dötsch, F. Bernhard, Advances in cell-free protein synthesis for the functional and structural analysis of membrane proteins, *New Biotech.* 28 (2011) 262-271.

- [18] F. Junge, B. Schneider, S. Reckel, D. Schwarz, V. Dotsch, F. Bernhard, Large-scale production of functional membrane proteins, *Cell. Mol. Life Sci.* 65 (2008) 1729-1755.
- [19] A.S. Spirin, V.I. Baranov, L.A. Ryabova, S.Y. Ovodov, Y.B. Alakhov, A continuous cell-free translation system capable of producing polypeptides in high yield, *Science* 242 (1988) 1162-1164.
- [20] K. Madin, T. Sawasaki, T. Ogasawara, Y. Endo, A highly efficient and robust cell-free protein synthesis system prepared from wheat embryos: Plants apparently contain a suicide system directed at ribosomes, *Proc. Natl. Acad. Sci. USA* 97 (2000) 559-564.
- [21] D.A. Vinarov, C.L.L. Newman, J.L. Markley, Wheat germ cell-free platform for eukaryotic protein production, *FEBS J* 273 (2006) 4160-416.
- [22] M. Aoki, T. Matsuda, Y. Tomo, Y. Miyata, M. Inoue, T. Kigawaa, S. Yokoyama, Automated system for high-throughput protein production using the dialysis cell-free method, *Prot. Express. Purif.* 68 (2009) 128-136.
- [23] T.H. Bayburt, Y.V. Grinkova, S.G. Sligar, Self-assembly of discoidal phospholipid bilayer nanoparticles with membrane scaffold proteins, *Nano Lett.* 2 (2002) 853-856.
- [24] I.G. Denisov, Y.V. Grinkova, A.A. Lazarides, S.G. Sligar, Directed self-assembly of monodisperse phospholipid bilayer nanodiscs with controlled size, *J. Am. Chem. Soc.* 126 (2004) 3477-3487.
- [25] H.D.T. Mertens, D.I. Svergun, Structural Characterization of proteins and complexes using small-angle X-ray solution scattering, *J. Struct. Biol.* 172 (2010) 128-141.
- [26] T. Sawasaki, Y. Hasegawa, M. Tsuchimochi, N. Kamura, T. Ogasawara, T. Kuroita, Y. Endo, Bilayer cell-free protein synthesis system for high-throughput screening of gene products, *FEBS Lett.* 514 (2010) 102-105.
- [27] M.D. Abramoff, P.J. Magalhaes, S.J. Ram, Image Processing with ImageJ. *Biophot. Int.* 11 (2004) 36-42.

- [28] J.E. Tropea, S. Cherry, D.S. Waugh, Expression and purification of soluble His₆-tagged TEV protease, *Meth. Mol. Biol.* 498 (2009) 297-307.
- [29] F.J.D. Alvarez, C. Orelle, A.L. Davidson, Functional reconstitution of an ABC transporter in nanodiscs for use in electron paramagnetic resonance spectroscopy, *J. Am. Chem. Soc.* 132 (2010) 9513-9515.
- [30] M.V. Petoukhov, D. Franke, A.V. Shkumatov, G. Tria, A.G. Kikhney, M.Gajda, C. Gorba, H.D.T. Mertens, P.V. Konarev, D.I. Svergun, New developments in the ATSAS program package for small-angle scattering data analysis, *J. Appl. Crystallogr.* 45 (2012) 342-350.
- [31] D.I.Svergun, Determination of the regularization parameter in indirect-transform methods using perceptual criteria, *J. Appl. Crystallogr.* 25 (1992) 495-503.
- [32] R.B. Kapust, J. Tözsér, J.D. Fox, D.E. Anderson, S. Cherry, T.D. Copeland, D.S. Waugh, Tobacco Etch Virus protease: mechanism of autolysis and rational design of stable mutants with wild-type catalytic proficiency, *Protein Eng* (2001)14, 993-1000.
- [33] E.M. Shematek, J.A. Braatz, E. Cabib, E. Biosynthesis of the yeast cell wall. I. Preparation and properties of (1,3)- β -glucan synthetase, *J. Biol. Chem.* 255 (1980) 888-894.
- [34] M. Hrmova, C.S. Taft, C.P. Selitrennikoff, (1,3)- β -D-Glucan synthase of *Neurospora crassa*: Partial purification and characterization of solubilized enzyme activity, *Exp. Mycol.* 13 (1989) 129-139.
- [35] Rath, A., Glibowicka, M., Nadeau, V.G., Chen, G., and Deber, C.M., Detergent binding explains anomalous SDS-PAGE migration of membrane proteins, *Proc. Natl. Acad. Sci. USA* 106 (2009) 1760-1765.
- [36] A. Nozawa, T. Ogasawara, S. Matsunaga, T. Iwasaki, T. Sawasaki, Y. Endo, Production and partial purification of membrane proteins using a liposome-supplemented wheat cell-free translation system, *BMC Biotechnol.* 11 (2011) 35-44.

- [37] I.G. Denisov, M.A. McLean, A.W. Shaw, Y.V. Grinkova, S.G. Sligar, Thermotropic phase transition in soluble nanoscale lipid bilayers, *J. Phys. Chem. B* 109 (2004) 15580-15588.
- [38] B.J. Baas, I.G. Denisov, S.G. Sligar, Homotropic cooperativity of monomeric cytochrome P450 3A4 in a nanoscale native bilayer environment, *Arch. Biochem. Biophys.* 430 (2004) 218-228.
- [39] O. Glatter, A new method for the evaluation of small-angle scattering data, *J. Appl. Crystallogr.* 10 (1977) 415-421.
- [40] N. Skar-Gislinge, J.B. Simonsen, K. Mortensen, R. Feidenhans. S.G. Sligar, B.L. Møller, T. Bjørnholm, L. Arleth, Elliptical Structure of phospholipid bilayer nanodiscs encapsulated by scaffold proteins: casting the roles of the lipids and the protein, *J. Am. Chem. Soc.* 132 (2010) 13713-13722.
- [41] C. Pasquier, V.J. Promponas, G.A. Palaios, J.S. Hamodrakas, A novel method for predicting transmembrane segments in proteins based on a statistical analysis of the SwissProt database: the PRED-TMR algorithm, *Protein Eng.* 12 (1999) 381-385.
- [42] G.S. Waldo, B.M. Standish, J. Berendzen, T.C. Terwilliger, Rapid protein-folding assay using green fluorescent protein, *Nat. Biotechnol.* 17 (1999) 691-695.
- [43] D. Drew, S. Newstead, Y. Sonoda, H. Kim, G. von Heijne, S. Iwata, GFP-based optimization scheme for the overexpression and purification of eukaryotic membrane proteins in *Saccharomyces cerevisiae*, *Nat. Protocols* 3 (2008) 784-798.
- [44] J.M. Hsieh, G.M. Besserer, M.G. Madej, H.-Q. Bui, S. Kwon, J. Abramson, Bridging the gap: A GFP-based strategy for overexpression and purification of membrane proteins with intra and extracellular C-termini, *Protein Sci.* 19 (2010) 868-880.
- [45] K. Mizutani, S. Yoshioka, Y. Mizutani, S. Iwata, B. Mikami, High-throughput construction of expression system using yeast *Pichia pastoris*, and its application to membrane proteins, *Protein Express. Purif.* 77 (2011) 1-8.

- [46] A. Deniaud, L. Liguori, I. Blesneac, J.L. Lenormand, E. Pebay-Peyroula, Crystallisation of the membrane protein hVDAC1 produced in cell-free system. *Biochim, Biophys. Acta - Biomembranes* 1798 (2010) 1540-1546.
- [47] L. Isaksson, J. Enberg, R. Neutze, B.G. Karlsson, A. Pedersen, Expression screening of membrane proteins with cell-free protein synthesis, *Prot. Express. Purif.* 82 (2012) 218-225.
- [48] P. Bazzacco, E. Billon-Deni, S. Sharma, L.J. Catoire, S. Mar, C. Le Bon, E. Point, J.-L. Banères, G. Durand, F. Zito, B. Pucci, J.-L. Popot, Nonionic homopolymeric amphipols: application to membrane protein folding, cell-free synthesis, and solution nuclear magnetic resonance, *Biochemistry* 51 (2012) 1416-1430.
- [49] N. Dowhan, Molecular basis for membrane phospholipid diversity, why are there so many lipids?, *Annu. Rev. Biochem.* 66 (1997) 199-232.
- [50] X. Zhao, Y. Nagai, P.J. Reeves, P. Kiley, H.G. Khorana, S. Zhang, Designer peptide surfactants stabilize diverse functional membrane proteins, *Chem. Soc. Rev.* 41 (2012) 1721-1728.
- [51] R. Yan, X. Mo, A.M. Paredes, K. Dai, F. Lanza, M.A. Cruz, R. Li, Reconstitution of the platelet glycoprotein Ib-IX complex in phospholipid bilayer nanodiscs, *Biochemistry* 50 (2011) 10598-10606.
- [52] M.T. Marty, A. Das, S.G. Sligar, Ultra-thin layer MALDI mass spectrometry of membrane proteins in nanodiscs, *Anal. Bioanal. Chem.* 402 (2012) 721-729.
- [53] Y. Ihara, T. Takeda, F. Sakai, Y. Hayashi, Transferase activity of GhCesA2 (putative cotton cellulose 4- β -glucosyltransferase) expressed in *Pichia pastoris*, *J. Wood Sci.* 48 (2002) 425-428.

Figure legends

Figure 1 SDS-PAGE of WG-CFPS translation reactions performed in bilayer mode and supplemented with DMPC liposomes (10 mg/ml) and mRNA of His-CrdS, His-Xa-CrdS and His-TEV-CrdS in lanes 1-3, respectively. Lane 4 contains the reaction lacking mRNA. The black arrows point to the synthesised CrdS proteins that migrate to a region of 56-60 kDa; theoretical masses of the CrdS proteins are between 73-76 kDa. St. indicates molecular mass standards.

Figure 2 SDS-PAGE and Western immuno-blot analyses of WG-CFPS translation reactions performed in bilayer mode and supplemented with DMPC (2.5 mg/ml) liposomes. Lanes 1 and 2 (duplicates) in the Coomassie stained panel A, and in the Western immuno-blot with the anti-CrdS antibody (panel B), contain translation reactions with His-TEV-CrdS mRNA, and lane 3 represents the reaction lacking mRNA. Lane 1 in the Western immuno-blot detected *via* alkaline phosphatase-conjugated streptavidin (panel C) contains the total WG-CFPS translation reaction, and lanes 2 and 3 represent separated pellet and supernatant fractions, respectively. The black arrows point to synthesised CrdS that migrate to a region of 56-60 kDa; CrdS theoretical mass is 73-76 kDa. St. indicates molecular mass standards.

Figure 3 Density gradient ultra-centrifugation of the CrdS proteo-liposomes made from DMPC. Western immuno-blot analysis was performed with the anti-CrdS antibody. Lanes 1-10 represent fractions collected after ultra-centrifugation. Lane 3 contains the fraction with CrdS that has successfully been incorporated in DMPC liposomes and lane 11 contains a non-fractionated WG-CFPS translation reaction mixture supplemented with the DMPC liposomes. The inset shows the membrane stained with Ponceau S. The black arrows point to synthesised CrdS that migrates to a region of 56-60 kDa; CrdS theoretical mass is 73-76 kDa. St. indicates molecular mass standards.

Figure 4 TEM of the DMPC liposomes with (panel A) and without (panel B) CrdS. The lines indicate sizes of 1 μm .

Figure 5 Yields of CrdS during WG-CFPS with of liposomes prepared from a variety of lipids. CrdS yields are given in mg/ml for liposomes prepared from DMPC (2.5-10 mg/ml), DOPC (2.5 mg/ml), POPC (5 mg/ml), DOPG:POPE=2:3 ratio by weight (5 mg/ml), asolectin (5 mg/ml) and the total extract of lipids from *E. coli* (5 mg/ml). The numbers in brackets indicate lipid concentrations that were optimal for WG-CFPS. No synthesis occurred with DOPG and DOTAP (data not shown). CrdS quantification was performed using the ImageJ software [27]. The standard errors are shown as vertical bars and were determined from three measurements.

Figure 6 SDS-PAGE analysis of WG-CFPS translation reactions performed in bilayer mode and supplemented with surfactants. Lanes 1 (supernatant and pellet fractions) contain reactions lacking mRNA. Lanes 2-7 (supernatants and pellets fractions) represent the His-TEV-CrdS mRNA reactions in the presence of digitonin, DM, DDM, Brij-58, Tween 80 and Triton X-100. The concentrations of surfactants used in WG-CFPS are listed in Table 2. Black arrows point to highest yields of synthesised CrdS. St. indicates molecular mass standards.

Figure 7 Anti-CrdS antibody Western immuno-blot analysis of WG-CFPS translation reactions performed in bilayer mode and supplemented with surfactant peptides. Lanes 1 and 2 represent reactions lacking mRNA, and with His-TEV-CrdS mRNA and 0.04% (w/v) Brij-58, respectively. Lanes 3-5, 6-8 and 9-11 contain the His-TEV-CrdS mRNA reactions in the presence of 1 mM, 2 mM and 4 mM Ac-AAAAAAD, 1 mM, 2 mM and 4 mM Ac-IIID and 1 mM, 2 mM

and 4 mM Ac-LLLK-NH₂, respectively. The black arrows point to highest yields of synthesised CrdS. St. indicates molecular mass standards.

Figure 8 SDS-PAGE analysis of WG-CFPS translation reactions performed through dialysis mode. Lane 1 represents the reaction lacking mRNA, lanes 2-4 contain the His-TEV-CrdS mRNA reactions with 0.04% (w/v) Brij-58 after 24 hours, 48 hours and 72 hours, respectively. The black arrows point to synthesised CrdS. St. indicates molecular mass standards.

Figure 9 SDS-PAGE analysis of CrdS purified *via* IMAC in the presence of 0.04% (w/v) Brij-58. Lane 1 contains a crude translation reaction before IMAC. Lane 2 shows unbound components collected as flow-through following incubation of the CFPS reaction with the Ni-NTA beads. Components removed during the 20 mM imidazole washing steps are shown in lanes 3-6. Lanes 7-12 indicate fractions eluted with 50 mM, 100 mM, 150 mM, 200 mM, 250 mM and 500 mM imidazole. Purity of the CrdS preparation shown in lane 11 was estimated to be between 50% and 60%. The black arrow points to purified CrdS. St. indicate molecular mass standards.

Figure 10 Reconstitution of CrdS in nanodiscs. Nanodisc assembly (from *E. coli* lipids or POPC and MSP1E3D1) proceeded as described in the Materials and methods section. Panel A, shows an elution profile of the CrdS nanodiscs during SEC on the Superdex 200 10/300 GL column. Full line, dashed and dotted traces indicate elution volumes of the CrdS nanodiscs prepared from the *E. coli* lipids (full line) or POPC (dashed line) and those of POPC empty nanodiscs (dotted line), respectively. In silver-stained SDS-PAGE (panel B), lane 1 contains 75 ng of BSA per lane, and lanes 2 and 3 represent the reconstituted CrdS nanodiscs made from the *E. coli* lipids and POPC, respectively. The respective top arrowheads and the bottom arrows point to CrdS and MSP1E3D1. A known amount of BSA in lane 1 (75 ng) was used to estimate protein concentration

of CrdS. Panel C, in Western immuno-blot detected with the anti 6xHis antibody, lane 1 contains IMAC-purified CrdS (white arrow), and lanes 2 and 3 represent the reconstituted CrdS nanodiscs made from the *E. coli* lipids and POPC, respectively. The arrowheads, bound by brackets in panels B and C, point to a diffused band of CrdS, respectively. The bottom arrow indicates MSP1E3D1. In panels B and C, St. indicates molecular mass standards. Panel D shows TEM images of the CrdS nanodiscs made from *E. coli* lipids (top panel) or POPC (bottom panel). White and black arrows show the clustered CrdS nanodiscs. A substantial proportion of CrdS nanodiscs is non-clustered. The lines corresponds to 100 nm.

Figure 11 SAXS of CrdS nanodiscs prepared from the *E. coli* or POPC lipids and MSP1E3D1. The SAXS profiles of the *E. coli* total lipid extract or POPC nanodiscs with reconstituted CrdS are indicated in black or blue circles, respectively. Inset shows regularised curves from the IFT fitting procedure used to generate the real space scattering density distribution functions, $p(r)$. Fits and density distributions of the *E. coli* lipids or POPC nanodiscs with reconstituted CrdS are shown as black and blue lines, respectively. The SAXS profiles are offset for clarity.

Table 1 Primers used for ligation-based cloning of the pEU-His-CrdS, pEU-His-Xa-CrdS and pEU-His-TEV-CrdS DNA fusions.

Construct	Primer	Sequence ^a
pEU-His-CrdS	5' Forward	CTCGAGAGTGCTGAAGGTGAC
	5' Reverse	GCGGCCGCTTATCCTCAGAATGCCCGTGCGAG
pEU-His-Xa-CrdS	5' Forward	CTCGAGATTGAAGGACGAAGTGCTGAACGTGAC
	5' Reverse	GCGGCCGCTTATCCTCAGAATGCCCGTGCGAG
pEU-His-TEV-CrdS	5' Forward	CTCGAGAGTGCTGAAGGTGAC
	5' Reverse	GCGGCCGCTTATCCTCAGAATGCCCGTGCGAG

^aBold types indicate the *XhoI* (forward) and *NotI* (reverse) restriction sites. The italicised and underlined sequences indicate the proteolytic Factor Xa site and the stop-Gly-stop motif, respectively.

The remainder of the sequences corresponds to coding regions of CrdS.

Table 2 Surfactants used during wheat germ cell-free synthesis of CrdS.

Surfactants	Short name	Final concentration	x CMC	Source ^a
<i>n</i> -Dodecyl- β -D-maltoside	DDM	0.8% (w/v)	12	Anatrace
<i>n</i> -Decyl- β -D-maltoside	DM	0.08% (w/v)	9.2	Anatrace
<i>n</i> -Octyl- β -D-glucopyranoside	β -OG	0.5% (w/v)	1.3	Anatrace
Digitonin		0.4% (w/v)	4.5	Sigma
Polyoxyethylene-(20)-cetyl-ether (C _{16/20})	Brij-58	0.04% (w/v)	4.7	Sigma
Polyoxyethylene-sorbitan-monolaurate 80	Tween 80	3% (v/v)	1.5	Sigma
Polyethylene-glycol-p-1,1,3,3-tetramethyl-butylphenyl-ether	Triton X-100	0.5% (v/v)	33.5	BDH
Nonylphenyl-polyethylene-glycol	NP40	0.5% (w/v)	1.3	Merck
3-[(3-Cholamidopropyl)dimethylammonio]-1-propansulfonate	CHAPS	0.5% (w/v)	1.8	Anatrace

^aThe sources are Anatrace (Santa Clara, CA, USA), Sigma (St. Louis, MO, USA), BDH Chemicals (Poole, Dorset, UK) and Merck Chemicals (Darmstadt, Germany).

Table 3 Lipids used for preparation of liposomes for wheat germ cell-free synthesis of CrdS.^aZ, A and C indicate zwitterionic, anionic and cationic lipids, respectively.

Lipid	Short name	Charge ^a	Structure
1,2-Dimyristoyl- <i>sn</i> -glycero-3-phosphocholine	DMPC	Z	
1-Palmitoyl-2-oleoyl- <i>sn</i> -glycero-3-phosphocholine	POPC	Z	
1,2-Dioleoyl- <i>sn</i> -glycero-3-phosphocholine	DOPC	Z	
1,2-Dioleoyl- <i>sn</i> -glycero-3-phospho-(1'- <i>rac</i> -glycerol)	DOPG	A	
1-Palmitoyl-2-oleoyl- <i>sn</i> -glycero-3-phosphoethanolamine	POPE	Z	
1,2-Dioleoyl-3-trimethylammonium-propane	DOTAP	C	
Asolectin	Asolectin	Z	Not applicable
<i>E. coli</i> total lipid extract	-	-	Not applicable

Table 4 Amino acid sequences of tryptic fragments of CrdS identified by MALDI-TOF/TOF.

CrdS tryptic peptides ^a
SIIAAQAMDYPR
TYCEAVGVNYVTRPDNK
VAVVQTPQFYFNSDPIQHNLGIDK
VFFDVFQPAK
WCLGTIQIGLLR
FGKEEMIGVDFR
ITGLSTENITLAAVPSSSDVKDVFVPEAGWMR

^aAmino acid sequences are indicated in a 1-letter code.

Table 5 (1,3)- β -D-Glucan synthase activity of CrdS prepared through wheat germ cell-free synthesis in the presence of surfactant Brij-58 and surfactant peptide Ac-AAAAAAD, and of CrdS co-translationally inserted in the *E. coli* total lipid extract liposomes, or reconstituted in the *E. coli* total lipid extract and POPC nanodiscs.

Sample	Specific activity (mU/mg protein) ^a
CrdS with Brij-58	0
CrdS with Ac-AAAAAAD	0.18 \pm 0.06
CrdS in <i>E. coli</i> lipid extract liposomes	0.22 \pm 0.05
CrdS in <i>E. coli</i> lipid extract nanodiscs	0
CrdS in POPC nanodiscs	0
Mixed membrane fraction of <i>S. cerevisiae</i>	1.97 \pm 0.07

^aA mean of two independent measurements.

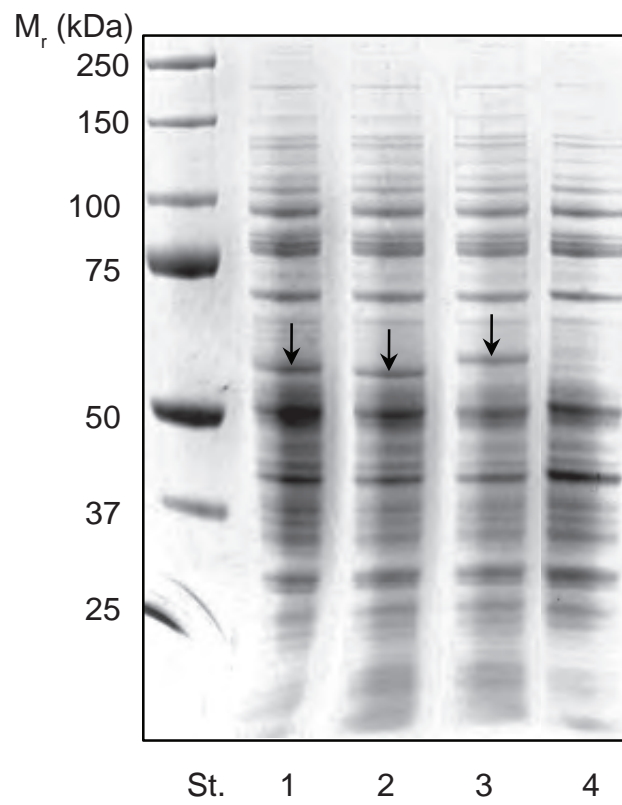


Figure 1

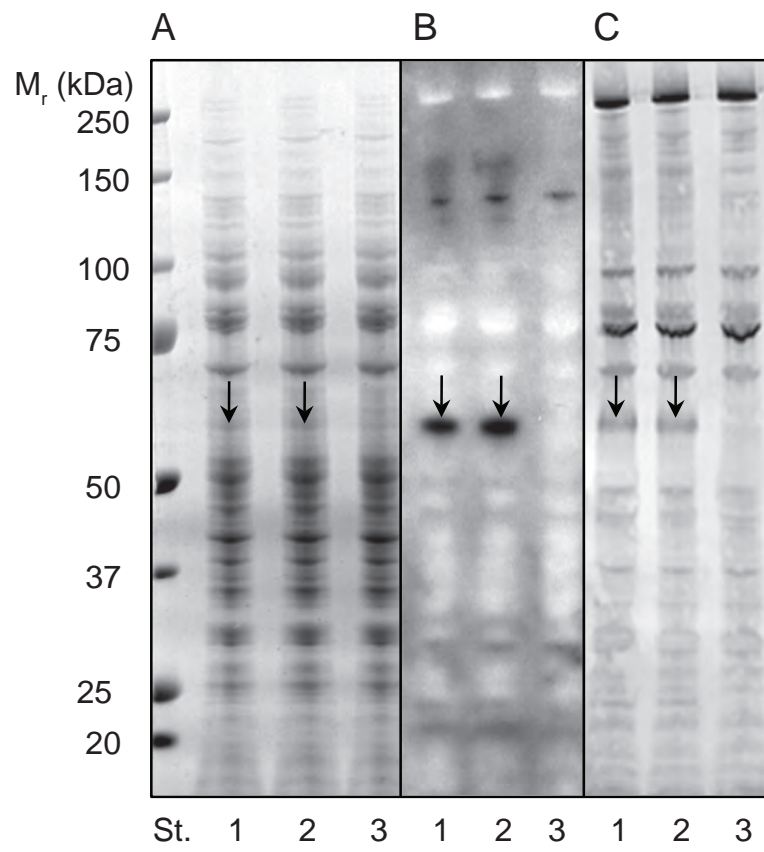


Figure 2

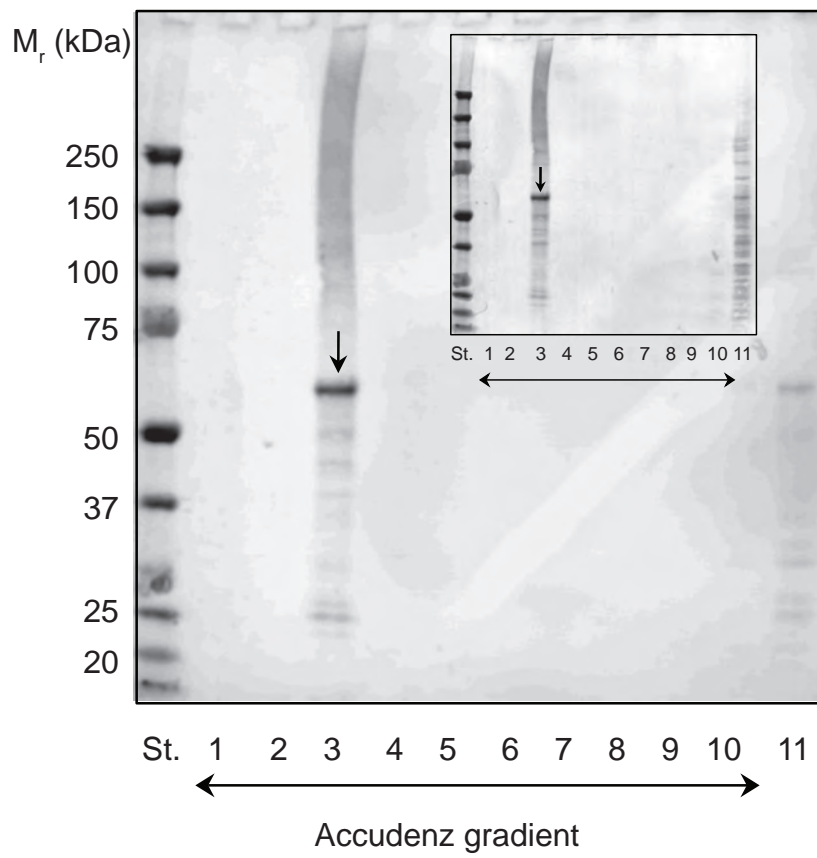


Figure 3

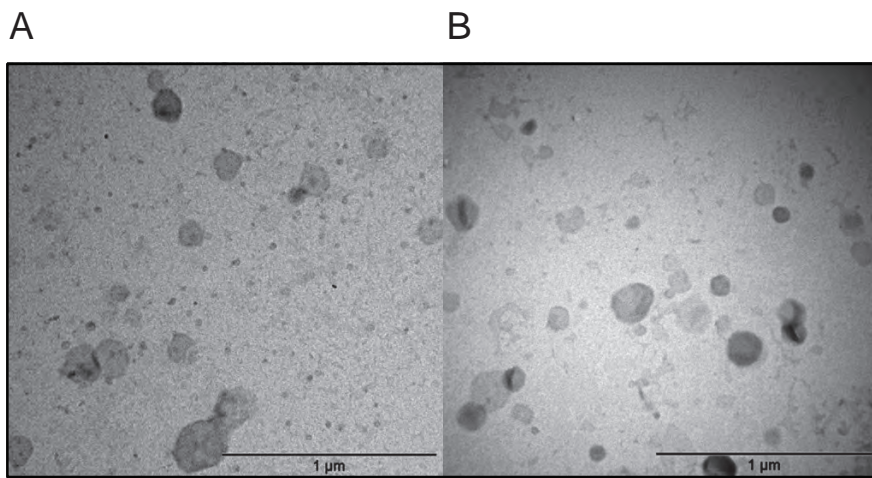


Figure 4

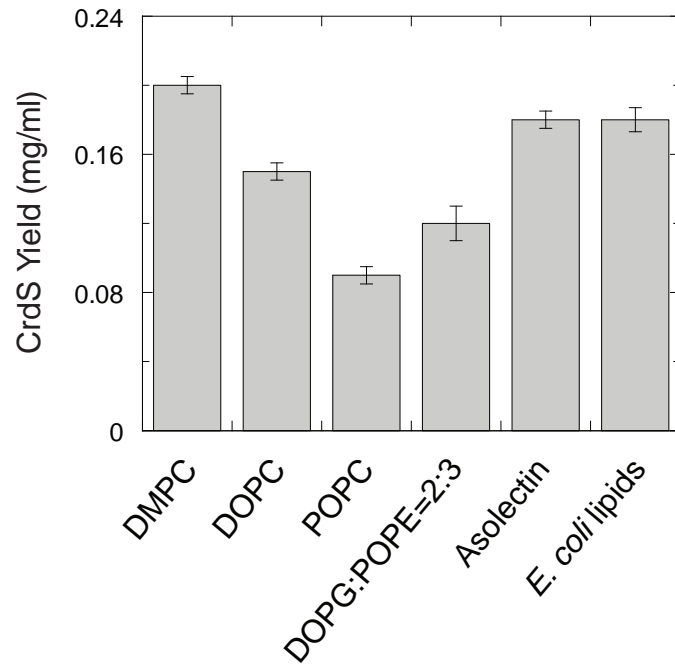


Figure 5

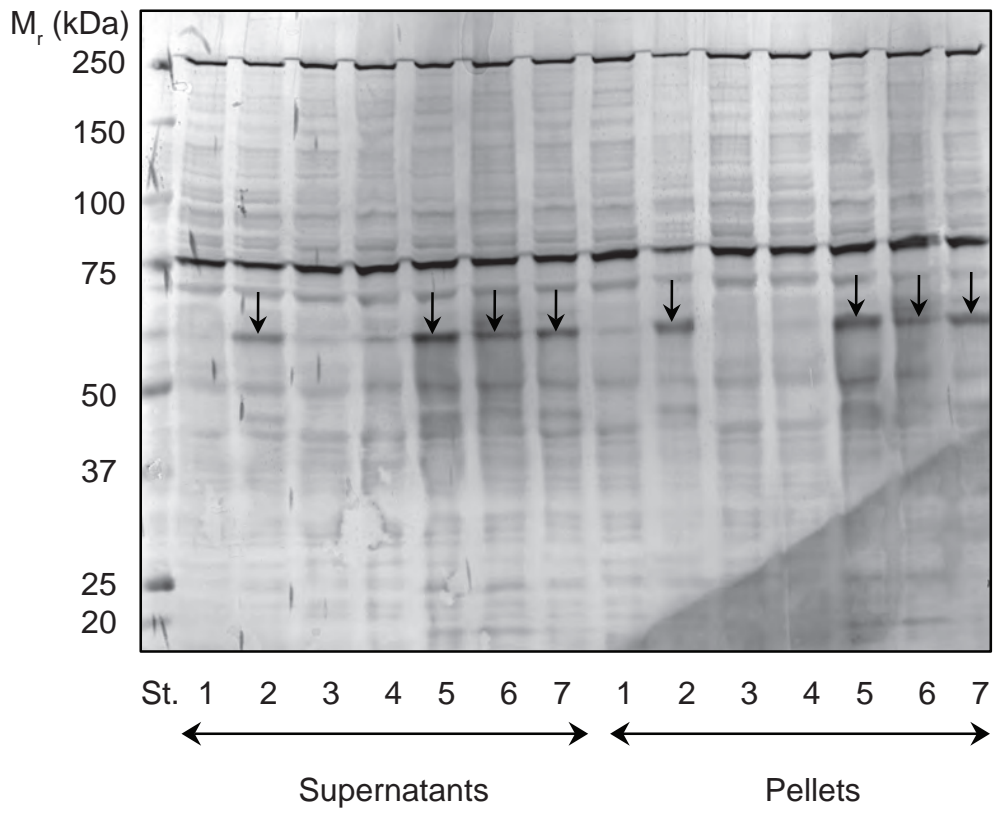


Figure 6

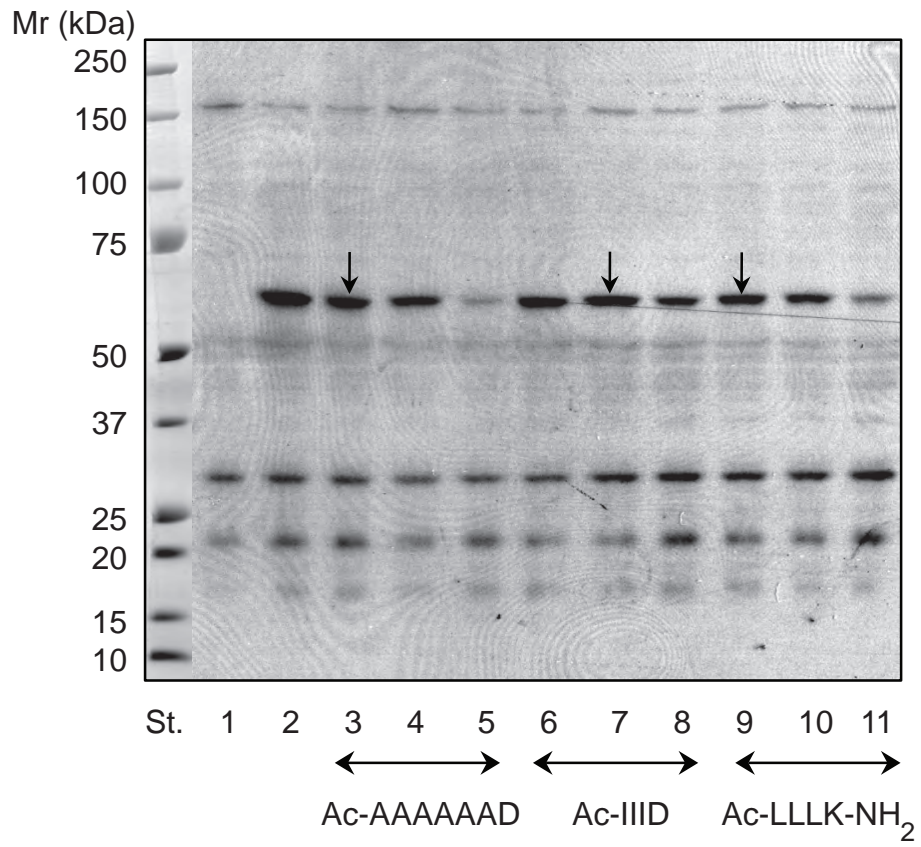


Figure 7

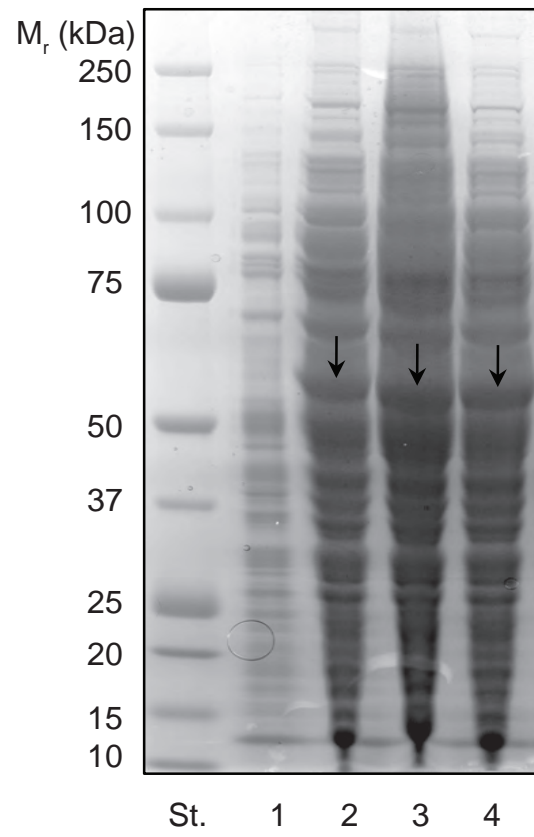


Figure 8

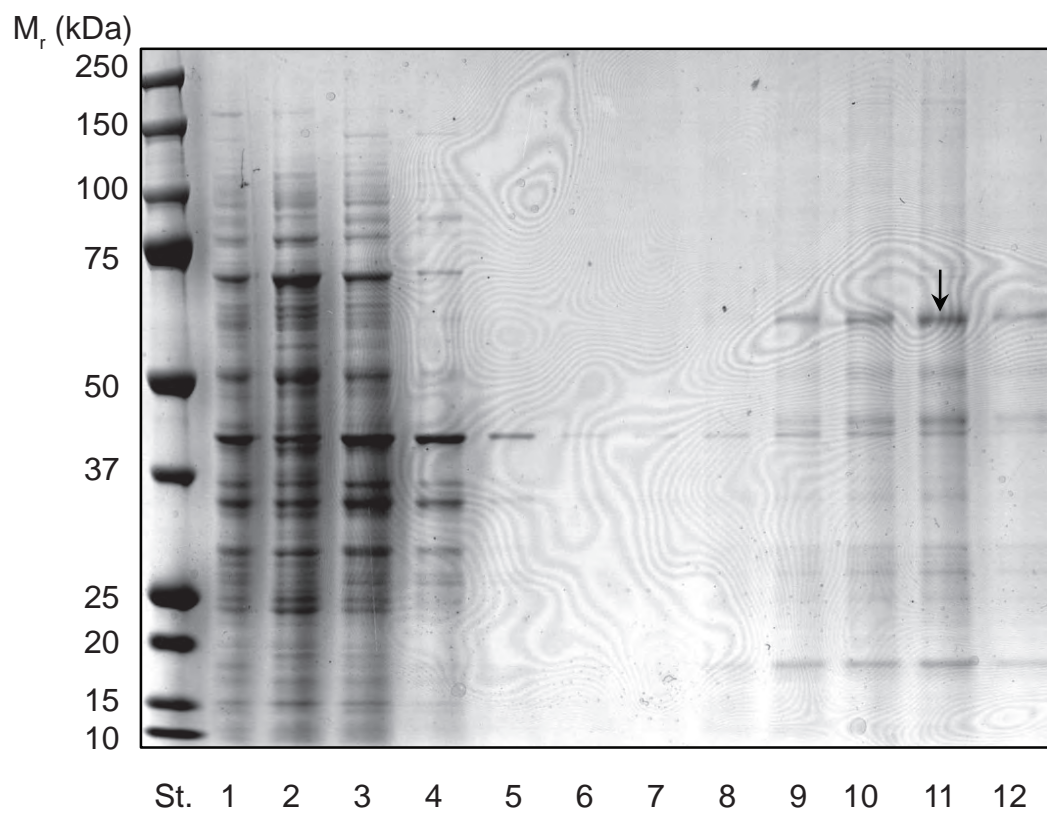


Figure 9

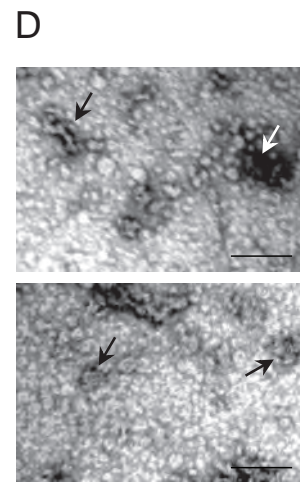
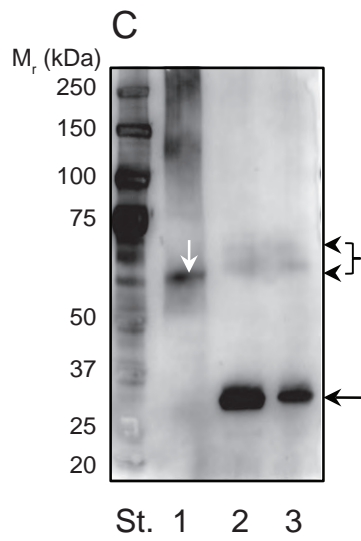
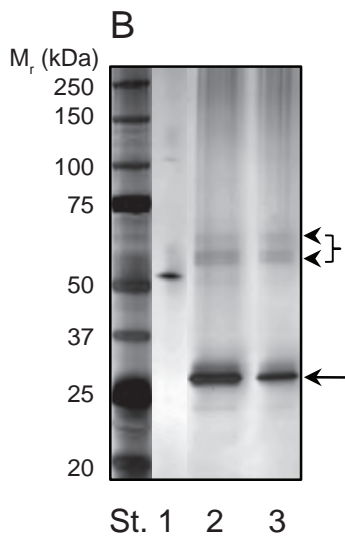
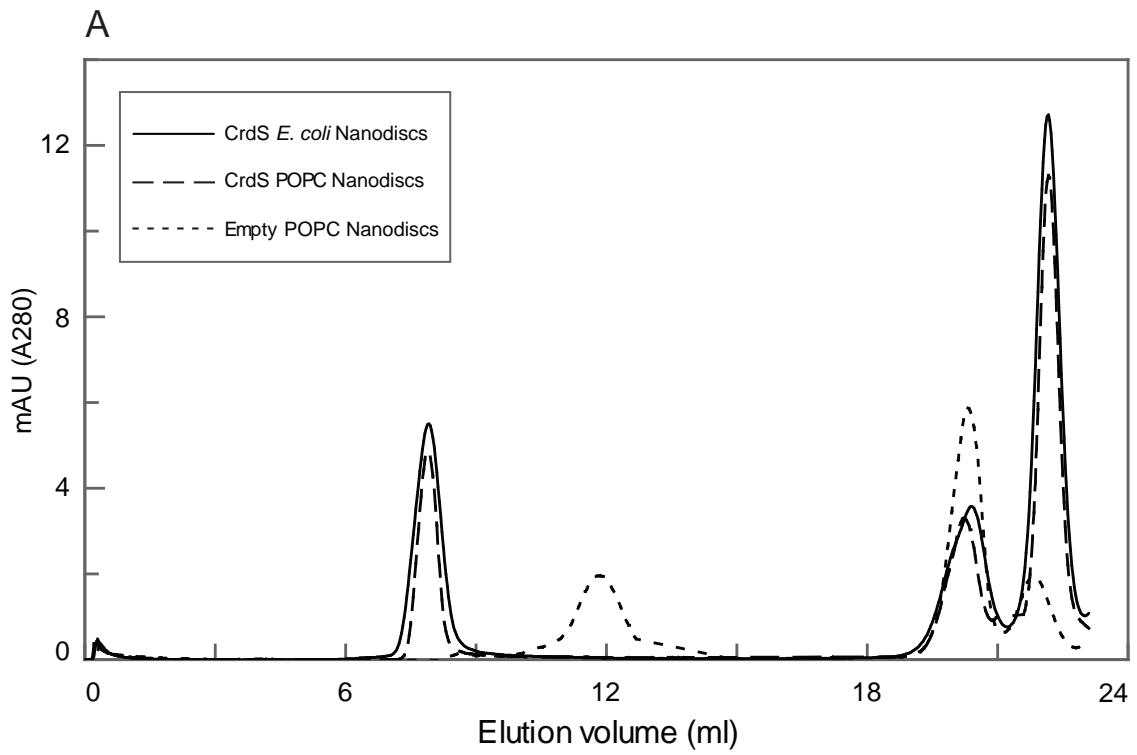


Figure 10

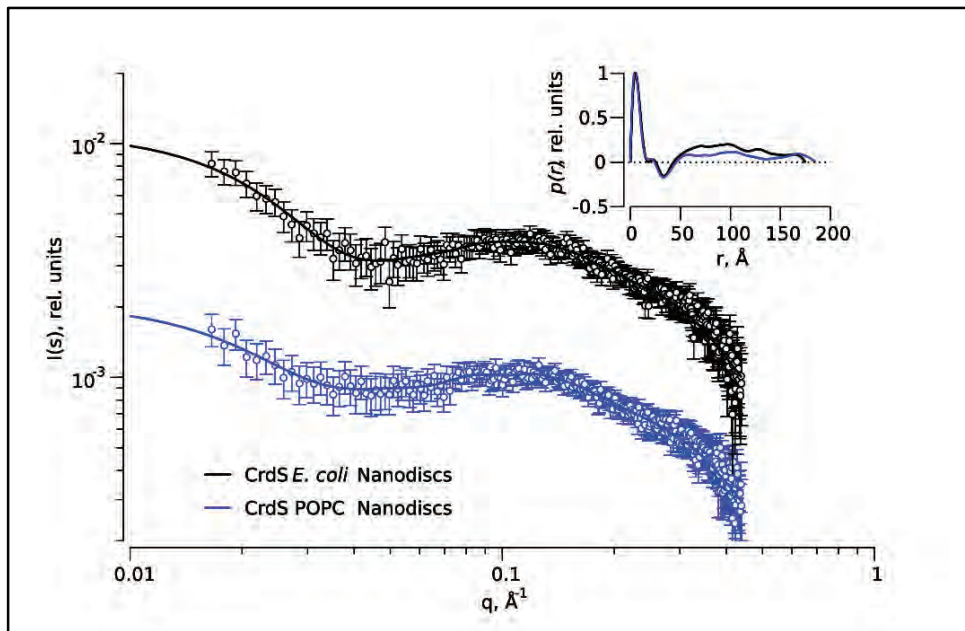


Figure 11